NUREG/IA-0209
NSI RRC KI 3067
IRSN-2002/33

International Agreement Report

Adaptation of USNRC's FRAPTRAN and IRSN's SCANAIR Transient Codes and Updating of MATPRO Package for Modeling of LOCA and RIA Validation Cases with Zr-1%Nb (VVER type) Cladding

Prepared by

A. Shestopalov, K. Lioutov, L. Yegorova
Nuclear Safety Institute of the Russian Research Centre "Kurchatov Institute"
Kurchatov Square 1, Moscow 123182, Russian Federation

April 2003

Prepared for
U.S. Nuclear Regulatory Commission, Institute for Radioprotection and Nuclear Safety (France), and Ministry of Science and Technologies of Russian Federation

Published by
U.S. Nuclear Regulatory Commission

AVAILABILITY OF REFERENCE MATERIALS IN NRC PUBLICATIONS

NRC Reference Material

As of November 1999, you may electronically access NUREG-series publications and other NRC records at NRC's Public Electronic Reading Room at http://www.nrc.gov/reading-rm.html. Publicly released records include, to name a few, NUREG-series publications; *Federal Register* notices; applicant, licensee, and vendor documents and correspondence; NRC correspondence and internal memoranda; bulletins and information notices; inspection and investigative reports; licensee event reports; and Commission papers and their attachments.

NRC publications in the NUREG series, NRC regulations, and *Title 10, Energy*, in the Code of *Federal Regulations* may also be purchased from one of these two sources.

1. The Superintendent of Documents
   U.S. Government Printing Office
   Mail Stop SSOP
   Washington, DC 20402–0001
   Internet: bookstore.gpo.gov
   Telephone: 202-512-1800
   Fax: 202-512-2250
2. The National Technical Information Service
   Springfield, VA 22161–0002
   www.ntis.gov
   1–800–553–6847 or, locally, 703–605–6000

A single copy of each NRC draft report for comment is available free, to the extent of supply, upon written request as follows:

Address: Office of the Chief Information Officer,
Reproduction and Distribution
Services Section
U.S. Nuclear Regulatory Commission
Washington, DC 20555-0001
E-mail: DISTRIBUTION@nrc.gov
Facsimile: 301–415–2289

Some publications in the NUREG series that are posted at NRC's Web site address http://www.nrc.gov/reading-rm/doc-collections/nuregs are updated periodically and may differ from the last printed version. Although references to material found on a Web site bear the date the material was accessed, the material available on the date cited may subsequently be removed from the site.

Non-NRC Reference Material

Documents available from public and special technical libraries include all open literature items, such as books, journal articles, and transactions, *Federal Register* notices, Federal and State legislation, and congressional reports. Such documents as theses, dissertations, foreign reports and translations, and non-NRC conference proceedings may be purchased from their sponsoring organization.

Copies of industry codes and standards used in a substantive manner in the NRC regulatory process are maintained at—

The NRC Technical Library
Two White Flint North
11545 Rockville Pike
Rockville, MD 20852–2738

These standards are available in the library for reference use by the public. Codes and standards are usually copyrighted and may be purchased from the originating organization or, if they are American National Standards, from—

American National Standards Institute
11 West 42nd Street
New York, NY 10036–8002
www.ansi.org
212–642–4900

Legally binding regulatory requirements are stated only in laws; NRC regulations; licenses, including technical specifications; or orders, not in NUREG-series publications. The views expressed in contractor-prepared publications in this series are not necessarily those of the NRC.

The NUREG series comprises (1) technical and administrative reports and books prepared by the staff (NUREG–XXXX) or agency contractors (NUREG/CR–XXXX), (2) proceedings of conferences (NUREG/CP–XXXX), (3) reports resulting from international agreements (NUREG/IA–XXXX), (4) brochures (NUREG/BR–XXXX), and (5) compilations of legal decisions and orders of the Commission and Atomic and Safety Licensing Boards and of Directors' decisions under Section 2.206 of NRC's regulations (NUREG–0750).

NUREG/IA-0209
NSI RRC KI 3067
IRSN-2002/33

International Agreement Report

Adaptation of USNRC's FRAPTRAN and IRSN's SCANAIR Transient Codes and Updating of MATPRO Package for Modeling of LOCA and RIA Validation Cases with Zr-1%Nb (VVER type) Cladding

Prepared by

A. Shestopalov, K. Lioutov, L. Yegorova
Nuclear Safety Institute of the Russian Research Centre "Kurchatov Institute"
Kurchatov Square 1, Moscow 123182, Russian Federation

April 2003

Prepared for
U.S. Nuclear Regulatory Commission, Institute for Radioprotection and Nuclear Safety (France), and Ministry of Science and Technologies of Russian Federation

Published by
U.S. Nuclear Regulatory Commission

ABSTRACT

The report presents the results of analytical work on updating and supplementing Zr-1%Nb (E110) cladding material property models as part of MATPRO package intended for joint use with thermal mechanical codes analyzing high burnup fuel transient behavior. The scope of work also included adapting U.S.NRC's FRAPTRAN code to the behavior analysis of fuel with E110 cladding (VVER type) and carrying out of the code assessment using selected experimental data. Satisfactory compliance of the results calculated by modified FRAPTRAN version with in-pile RIA and out-of-pile LOCA simulated test results is obtained. The obtained calculation data have been also compared with the predictions of the FRAP-T6 (U.S.NRC) and SCANAIR (IRSN, France) codes modified earlier.

TABLE OF CONTENTS

LIST OF FIGURES

LIST OF TABLES

FOREWORD

A world-wide trend to substantially increase nuclear fuel burnup to higher levels has led a number of countries, including the United States, to evaluate the effects of higher burnup on fuel behavior. Reactivity-initiated accident experiments, performed in France and Japan, have shown that fuel damage under these conditions may occur well below the threshold criteria used by various regulatory bodies, including the U.S. Nuclear Regulatory Commission (NRC). Questions have also been raised about the adequacy at high burnup of other fuel damage criteria used in safety analyses.

Consistent with the NRC's mission strategy to evaluate and resolve safety issues, the Office of Nuclear Regulatory Research is conducting a thorough investigation of high-burnup effects on fuel behavior. As part of this investigation, we recognized the value of a reactivity-initiated accident test program conducted by the Russian Research Center (Kurchatov Institute). In cooperation with the French Institute for Radioprotection and Nuclear Safety (IRSN) and the Russian nuclear industry, NRC now sponsors high-burnup fuel behavior work at the Kurchatov Institute. This includes in-reactor experiments, measurements of mechanical properties of irradiated cladding, and modification to the IRSN and NRC fuel behavior codes used to analyze fuel response to accident conditions.

The NRC participates in several experimental and analytical programs in order to gain a more complete understanding of highly irradiated fuel behavior under accident conditions. Among these programs, the work conducted at the Kurchatov Institute is significant. The ultimate goal of these activities is the development of new regulatory criteria for high-burnup fuel under design-basis accident conditions. However, the work has become even more relevant to safety considerations, in both France and the U.S., due to the introduction of the niobium-bearing zirconium alloys, which are similar to the alloys currently used in the Russian program. A portion of the Russian analytical work is described in the following report

Farouk Eltawila, Director
Division of Systems Analysis and Regulatory Effectiveness
Office of Nuclear Regulatory Research
U.S. Nuclear Regulatory Commission

LIST OF ACRONYMS

BIGR	Impulse Graphite Reactor (Russia)
CHF	Critical Heat Flux
FGR	Fission Gas Release
FRAPCON-3	NRC's steady-state fuel rod behavior code
FRAP-T6	NRC's transient fuel rod behavior code
FRAPTRAN	NRC's transient fuel rod behavior code
HGR	Heat Generation Rate
HTC	Heat Transfer Coefficient
IGR	Impulse Graphite Reactor (Kazakhstan)
IRSN	Institute for Radioprotection and Nuclear Safety (France)
LOCA	Loss-of-Coolant Accident
LWR	Light Water Reactor
MATPRO	Library of material properties for LWR accident analysis, version 11, revision 1 (USA)
NSI RRC KI	Nuclear Safety Institute of Russian Research Centre "Kurchatov Institute" (Russia)
NV NPP	NovoVoronezh nuclear power plant
PNNL	Pacific Northwest National Laboratory
PWR	Pressurized Water Reactor
RIA	Reactivity Initiated Accident
RIAR	State Research Centre "Research Institute of Atomic Reactors" (Russia)
SCANAIR	French IRSN's transient fuel rod behavior code
TRIFOB	Code for calculation of isotopic composition (Russia)
NRC	U.S. Nuclear Regulatory Commission
VVER	Russian type of pressurized water reactor

1. INTRODUCTION

At present, activities related to developing and updating thermal mechanical computer codes for LWR fuel behavior modeling in the broad range of possible emergency modes and achieved burnup values are being intensively carried out. Steady tendency toward increasing burnup in commercial reactor sets forth corresponding requirements for quality of the fuel rod behavior codes intended for high burnup fuel analysis in design-basis accidents. This issue took on additional actuality in connection with consideration of alternative types of fuel claddings with high performance up to high burnup values.

Claddings of zirconium-niobium E110 alloy that are used in Russian pressurized water reactors of VVER type show high resistance to oxidation and hydriding during base irradiation when burnup of 50 MWd/kgU and higher are reached [1, 2]. Along with low corrosion, highly irradiated E110 claddings show high residual ductility, which is verified by the pulse experiment results at IGR and BIGR reactors and by the mechanical test data [3, 4, 5]. Thus, claddings of such an alloy type are of interest as candidates for fuel with high burnup limit. As a result, the main task of the presented work was to expand the domains of applicability of the specified codes, which were Zircaloy cladding-oriented initially, toward alternative fuel analysis.

Work with fuel rod behavior codes conducted at NSI RRC KI since 1996 was focused upon implementation of material property models for Zr-1%Nb cladding in NRC's FRAP-T6 and French IRSN's SCANAIR transient codes and upon adaptation of the codes for calculating validation cases. The latter include in-pile and out-of-pile experiments with fuel rods of VVER type.

Providing the codes with the Zr-1%Nb cladding material property package was the first important stage of work. Earlier, in the course of adapting FRAP-T6 and SCANAIR codes, a package of the main thermal and mechanical properties of the E-110 claddings was developed in MATPRO format [6, 7]. It needs to be emphasized that a special experimental program was initiated jointly by NSI RRC KI and RIAR to measure mechanical properties of unirradiated and irradiated claddings in the broad range of temperatures and strain rates [3, 8]. Later on the results of the new mechanical tests allowed to update the mechanical properties database [5, 9, 10]. Obtaining of the new test data coincided timewise with the issue of the first version of FRAPTRAN code developed by PNNL per request of NRC [11]. Therefore the updated correlations for cladding plastic deformation presented in the present report were implemented in MATPRO package to be used already with FRAPTRAN and SCANAIR codes.

During the next stage, calculations of the selected RIA and LOCA validation cases with fuel rods of VVER type were conducted. The main objective of these calculations was to analyze accuracy of predictions by FRAPTRAN code of the most important thermal and mechanical parameters of the fuel with Zr-1%Nb cladding, as well as to check performance of the mechanical model with the new characteristics in different cladding loading modes. In order to model the validation cases correctly, modifications of the original FRAPTRAN version were needed aside from the updating of the material property package. Mainly, the modifications were stipulated for by the design of the fuel rods of VVER type (central hole in the fuel pellet) and by specificities of clad-to-coolant heat transfer in pulse tests. In addition to that, a number of coding problems were resolved including adding of new global and local variables and correcting a few bugs and inaccuracies in the as-received version of FRAPTRAN code.

Accumulated experience in modeling fuel rods with Zr-1%Nb claddings using FRAP-T6 and SCANAIR codes, as well as the analysis of the first FRAPTRAN validation calculations allowed us to draw some generalized conclusions on quality of predictions by the code of behavior of a fuel rod with alternative cladding. Based on calculation results for high burnup fuel under power pulse conditions, proposals on future development of FRAPTRAN code were also presented in the report. They have to do with correct accounting of high burnup effects when analyzing fuel behavior in RIA.

2. ZR-1%NB CLADDING DATA BASE IMPLEMENTED IN MATPRO

Correlations of Zr-1%Nb (E110) cladding material properties, which were incorporated in MATPRO package, can be attributed to three main blocks:

- basic thermal properties;
- mechanical properties;
- high temperature oxidation kinetics.

Formally, to model fuel rods of VVER type in the most correct manner, large number of properties of cladding and fuel pellets should be reviewed and implemented in MATPRO as an alternative to the properties of western Zircaloy cladding and ceramic fuel. However, analysis of full range of accountable properties (including sensitivity study) conducted earlier [3] allowed to limit the number of key correlations for Zr-1%Nb necessary for implementation in MATPRO. As to the properties of UO_2 pellets, the difference between PWR and VVER types of fuel were found to be insignificant. This gave occasion not to duplicate original MATPRO correlations of material properties of the fuel. It should be mentioned here that this approach was also used, in particular, for thermal conductivity of fuel in burnup function. Earlier, during the process of modifying FRAP-T6 code for analysis of high burnup VVER fuel rods [6], limited published data were used for modeling degradation of thermal conductivity of fuel vs. burnup increase. At that time, appropriate model in MATPRO-V11 was not available. Recently developed FRAPTRAN code began to use new FRAPCON-3 thermal conductivity model [12], which takes burnup effects into account. This model was decided to be used in calculations of VVER fuel. Thus, within the framework of this activity in the course of modification of MATPRO package, primary attention was focused on material properties of Zr-Nb cladding.

2.1. Zr-1%Nb cladding thermal properties

Correlations of thermal properties of Zr-1%Nb cladding, incorporated in MATPRO package were taken from available publications of domestic analysts. Table 1 contains a set of applicable correlations and constants with references to source publications and routines of MATPRO package modified for calculations of fuel rods with E110 claddings.

Table 1. Zr-1%Nb cladding thermal properties implemented in MATPRO package.

Parameter, units	Nomenclature	Routine	Ref.
Thermal conductivity λ =[W/m K] $\lambda=15.0636\exp(0.4618\cdot10^{-3}T)$	T- temperature (K)	CTHCON	[13]
Specific heat C_P=[J/kg K] Slow heat up rate < 0.02 K/s (Table 2) Fast heat up rate > 1000 K/s (Table 3)	T- temperature (K)	CCP	[13, 14]
Enthalpy H=[J/g] $E=\int_{293}^{Tcurr} C_P dT$ Slow heat up rate < 0.02 K/s (C_p from Table 2) Fast heat up rate > 1000 K/s (C_p from Table 3)	T- temperature (K); T_{curr}- current temperature (K)	CCINP	[13, 14]

Parameter, units	Nomenclature	Routine	Ref.
Linear thermal expansion ε_{th}=[m/m] T< 573	ε_θ - thermal expansion in hoop direction (m/m)	CTHEXP	[3, 6, 13]
$\varepsilon_z=0.1338985 \cdot 10^{-8} T^2+3.85875 \cdot 10^{-6} T-0.127813365 \cdot 10^{-2}$	ε_z - thermal expansion in axial direction (m/m)		
$\varepsilon_\theta = 0.3336985 \cdot 10^{-8} T^2+5.65390 \cdot 10^{-6} T-0.199649865 \cdot 10^{-2}$	T- temperature (K)		
$573 \le T < 883$			
$\varepsilon_z=0.13725577 \cdot 10^{-2}+5.4\ 10^{-6}(T-573)$			
$\varepsilon_\theta=0.3336985 \cdot 10^{-8} T^2 + 5.6539 \cdot 10^{-6} T - 0.19965 \cdot 10^{-2}$			
$883 \le T < 1153$			
$\varepsilon_z=3.0465577 \cdot 10^{-3}+2.312 \cdot 10^{-8}(T-883) - 7.358 \cdot 10^{-8}(T-883)^2+1.7211 \cdot 10^{-10}(T-883)^3$			
$\varepsilon_\theta=5.5977 \cdot 10^{-3}+2.312 \cdot 10^{-8}(T-883)-7.358 \cdot 10^{-8}(T-883)^2+1.7211 \cdot 10^{-10}(T-883)^3$			
$T \ge 1153$			
$\varepsilon_z=1.076459 \cdot 10^{-3}+9.7\ 10^{-6}(T-1153)$			
$\varepsilon_\theta=3.627600 \cdot 10^{-3}+9.7\ 10^{-6}(T-1153)$			
Density, ρ=[kg/m^3] $\rho(T=293) = 6550$	ρ - density (kg/m^3)	INTINP	[15]
Melting point, T_{melt} =[K] $T_{melt} = 2133$	T_{melt} – melting temperature (K)	PHYPRP	[15]
Heat of fusion H_{fus} =[J/g] $H_{fus}=210$	H_{fus} – heat of fusion (J/g)	PHYPRP	[15]
Phase transition temperatures T_i=[K] $T_{\alpha \to \alpha+\beta}=883$, $T_{\alpha+\beta \to \beta}=1153$		PHYPRP	16
Meyer micro-hardness, H_M=[MPa]	T- temperature (K)	CMHARD	[16, 17]
T<800 K			
$H_M=2172.1 - 10.7055 \cdot T + 0.02765 \cdot T^2 - 3.278\ 10^{-5} \cdot T^3+ 1.423 \cdot 10^{-8} \cdot T^4$			
T≥800 K			
$H_M = \exp(26.034 - 0.026394 \cdot T + 4.3502 \cdot 10^{-5}\ T^2 - 2.5621 \cdot 10^{-8}\ T^3)$			

Table 2. Specific heat vs. temperature under slow heat up rate [13].

Parameter	Temperature (K)														
	393	473	573	673	773	873	883	973	1025	1073	1153	1173	1200	1300	1400
Specific heat (J/kg K)	345	360	370	380	383	385	448	680	816	770	400	392	392	393	393

Table 3. Specific heat vs. temperature under fast heat up rate [13].

$C_p = 237.5 + 15.91 \cdot 10^{-2} T$, [J/kg K] $500 < T < 1050$ K

$C_p = 199.7 + 12.364 \cdot 10^{-2} T$, [J/kg K] $1200 < T < 1600$ K

Parameter	Temperature (K)										
	1110	1120	1134	1142	1155	1161	1168	1177	1180	1090	1200
Specific heat, (J/kg K)	420	480	600	1000	1600	1400	1000	600	400	360	348

2.2. Zr-1%Nb cladding mechanical properties

Due to the difference in chemical composition and heat treatment, strength and ductility properties of as-received claddings of Zircaloy and Zr-1%Nb type are significantly different, especially at low and medium temperatures. In the case of highly irradiated cladding, difference in the levels of oxidation and hydrogenation results in fundamentally different mechanical behavior of these claddings under accident conditions. That is why incorporation of mechanical properties of both unirradiated and irradiated Zr-1%Nb claddings was considered the key task in modifying the material property package for transient codes.

In the framework of such a task, the program on development of a modern database on mechanical properties of the cladding used in the Russian pressurized water reactors of VVER type was initiated in NSI RRC KI at the end of the 1990s. Direct adaptation of the obtained data to the code algorithm requirements was an inseparable component of the program.

In the course of the program implementation [3], the main emphasis was made on studying of the properties important from the fast accidental processes point of view. Reactivity initiated accidents (RIA) and early stages of loss-of-coolant accidents (LOCA) can be considered among such processes. High strain rates, intensive stress growth in the cladding and a wide range of cladding temperatures can be considered general particularities of the cladding loading for these modes. Therefore, the main varied test parameters were the temperature and the strain rate.

Two types of claddings were tested in the framework of the program: as-received claddings and claddings of commercial fuel rods with the burnup of about 50 MWd/kg U.

The following kinds of tests were conducted with the cladding specimens:

- uniaxial tensile tests in transverse and rolling direction;
- biaxial tube burst tests with various biaxiality stress ratios.

The uniaxial tests were aimed at obtaining plastic deformation law parameters versus test conditions, and cladding failure criteria were the objective of the biaxial burst tests. As a result of the initial stages of the experimental program, the first version of the modified MATPRO package was acquired and used with FRAP-T6 (modified) and SCANAIR codes for analyzing high burnup VVER fuel [6, 7].

The last result of the mechanical tests (uniaxial tension in rolling direction and low temperature biaxial tension), which were reported in [5, 9, 10], allowed us to generalize the accumulated data and update correlations for the plastic deformation law parameters. The most important result of the test program was the anisotropy factors vs. temperature for unirradiated and irradiated cladding. The anisotropy factors allowed us to derive deformation laws in terms of effective stress-effective strains, which seems to be more correct for anisotropic claddings of Zr-based alloys. The other important thing was an extension of the temperature range for the cladding failure criterion in the form of the true hoop stress at rupture. Thus, this section presents the updated mechanical property correlations implemented in the MATPRO package (See Table 4-Table 6). Table 4 contains a set of correlations of Zr-1%Nb cladding elastic properties – Poisson's ratio, elastic and shear moduli taken from the literature.

Table 4 also shows dependencies of Zr-1%Nb alloy high-temperature creep rate on the temperature and the stress obtained in the unirradiated cladding samples [18]. These dependencies are incorporated into the newly developed MATPRO module CREEPS (See Section 4), because the original version of the package does not contain correlations for high-temperature cladding creep.

The implemented Zr-1%Nb alloy creep model takes into consideration, along with the temperature and the stress level, volumetric ratio of α and β phases in phase transition area. Corresponding test data obtained for equilibrium conditions are shown on Fig. 1. It is necessary to note that a literature search for the data on the effect of heating/cooling rates upon phase transition temperatures of the alloy produced no results. At the same time it is known that high cladding temperature variation rates typical for accidents shift $\alpha \rightarrow \beta$ transition boundaries. Effect of the heating rate upon annealing dynamics of irradiation-induced damages should also be taken into account in predicting mechanical response of irradiated claddings. Therefore, temperature dependencies of the main thermal and mechanical properties obtained mainly in thermodynamic equilibrium conditions may require updating. Such updating is a subject of future activities related to incorporating of heating/cooling rate into the set of the key test parameters.

It should repeat that currently the modified MATPRO package contains the cladding mechanical properties for only two levels of burnup – 0 (as-fabricated) and 50 MWd/kgU. Obtaining the continuous dependencies on burnup or fast neutron fluence was out of frame of the test program. However, basing on limited literature data [1, 19] one can preliminarily assume that presented here correlations for irradiated E110 cladding are applicable for burnup higher than 10 – 15 MWd/kgU. Additional work is needed to confirm such assumption and to obtain quantitative estimations of burnup dependence.

Table 4. Mechanical properties of Zr-1%Nb cladding.

Parameter, units	**Nomenclature**	**Routine**	**Ref.**
Elastic modulus, E=[MPa] 273 K<T≤1073 K $E=1.121\cdot10^5-64.38T$ 1073 K<T≤1273 K $E=9.129\cdot10^4-45.0T$	T- temperature (K)	CELMOD	[13]
Poisson's ratio, ν = [unitless] T<1273 $\nu= 0.42628-5.556\cdot10^{-5}T$	T- temperature (K)	CSHEAR, CLADF, COUPLE	[13]
Shear modulus, G = [MPa] T<1273 K $G=\frac{E}{2\cdot(1+\upsilon)}$	T- temperature (K); ν - Poisson's ratio (unitless); E – elastic modulus (GPa)	CSHEAR	-
Plastic deformation equation $\sigma = K\varepsilon^n\left(\frac{\dot\varepsilon}{\dot\varepsilon_o}\right)^m$ (see Table 5)	σ – true effective stress (MPa); K – strength coefficient (MPa); ε – true effective strain (unitless); n – strain hardening exponent (unitless); $\dot\varepsilon$ – current strain rate (1/s); $\dot\varepsilon_o$ – basic strain rate (1/s); $\dot\varepsilon_o=10^{-3}$ 1/s; m – strain rate sensitivity exponent (unitless)	CKMN	[10]

Parameter, units	Nomenclature	Routine	Ref.
Mechanical limits S_{ut} S_y δ_t δ_u calculated by MATPO equations with parameters of plastic stress-strain curve True hoop stress at burst σ_B = [MPa] 293≤T≤723 unirradiated $\sigma_B = 2016.268 - 5.2948\,T + 0.00627\,T^2 - 2.8233 \cdot 10^{-6}\,T^3$ 423≤T≤723 irradiated $\sigma_B = 4178.356 - 12.894\,T + 0.0154\,T^2 - 6.5545 \cdot 10^{-6}\,T^3$	S_{ut} – engineering ultimate strength (MPa); S_y – engineering yield stress (MPa); δ_t – total elongation (%); δ_u – uniform elongation (%);	CMLIMT	[3,10]
973<T≤1190 $\sigma_B = 116139.02 \exp(-0.0065753\,T)$ 1190<T≤1473 $\sigma_B = 7611.82 \exp(-0.004283\,T)$	T- temperature (K);		
Anisotropy coefficients of Hill's equation, F, G, H =[unitless] $\sigma_e = \left\{F(\sigma_\theta - \sigma_z)^2 + G(\sigma_z - \sigma_r)^2 + H(\sigma_r - \sigma_\theta)^2\right\}^{0.5}$ (see Table 6)	σ_e – effective clad stress (MPa); σ_θ – hoop clad stress (MPa); σ_z – axial clad stress (MPa); σ_r – radial clad stress (MPa)	CANISO	[10]
High-temperature creep strain rate, ε=[m/m] 1. T<883 K • $\sigma_e = 9 \div 32$: $\dot{\varepsilon} = 7.1 \cdot 10^5 \sigma_e^{2.2} \exp(-28900/T)$, • $\sigma_e = 32 \div 90$: $\dot{\varepsilon} = 26\,\sigma_e^{5.1} \exp(-28900/T)$, • $\sigma_e > 90$: $\dot{\varepsilon} = 2 \cdot 10^9 \exp(0.05\sigma_e)\exp(-28900/T)$. 2. T>1173 K $\dot{\varepsilon} = 0.09\,\sigma_e^{3.5} \exp(-13200/T)$, 3. 883 ≤ T < 1070 K $\sigma = f_\alpha \sigma_\alpha + f_\beta \sigma_\beta$, 4. 1070 ≤ T ≤ 1173 K $\varepsilon = f_\alpha \varepsilon_\alpha + f_\beta \varepsilon_\beta$	σ_e – effective clad stress (MPa) $\dot{\varepsilon}$ - effective creep strain rate (1/s) T- temperature (K) f_α, f_β -normalized volume fraction of α- and β- phase respectively (unitless) σ_α, σ_β - effective stress in α- and β- phase respectively (MPa) ε_α, ε_β - creep strain rate in α- and β- phase respectively (1/s)	CREEPS	[18]

Table 5. Parameters of plastic deformation equation versus temperature and cladding type.

<table>
<tr><th rowspan="2">Parameter</th><th colspan="2">Type of cladding</th></tr>
<tr><th>Unirradiated</th><th>Irradiated</th></tr>
<tr><td rowspan="5">Strength coefficient (MPa)</td><td>293<T≤797.9 K</td><td>293<T≤763 K</td></tr>
<tr><td>$K = 898.3710095 - 1.911883946 \cdot T + 0.002024675204 \cdot T^2 - 9.628259856 \cdot 10^{-7} \cdot T^3$</td><td>$K = 916.8547193 - 0.6046334417 \cdot T - 0.0002474820043 \cdot T^2$</td></tr>
<tr><td>797.9<T≤1223 K</td><td>763<T≤859.4 K</td></tr>
<tr><td rowspan="2">$K = \exp(-0.005608069738 \cdot T) \cdot 15180.65748$</td><td>$K = \exp(-0.00965027547 \cdot T) \cdot 491246.9131$</td></tr>
<tr><td>859.4<T≤1223 K
$K = \exp(-0.005608069738 \cdot T) \cdot 15180.65748$</td></tr>
</table>

Parameter	Type of cladding	
	Unirradiated	Irradiated
Strain hardening exponent (unitless)	$293<T\leq1223$ K	$293<T\leq759$ K
	$n = 0.04628421012 + 0.000197951907\cdot T - 3.314868215\cdot10^{-7}\cdot T^2 + 1.3913294\cdot10^{-10}\cdot T^3$	$n = -0.1255447757 + 0.001350416112\cdot T - 3.536814687\cdot10^{-6}\cdot T^2 + 3.734672258\cdot10^{-9}\cdot T^3 - 1.365014312\cdot10^{-12}\cdot T^4$
		$759<T\leq879$ K
		$n = -0.239614587 + 0.002839248035\cdot T - 8.226160457\cdot10^{-6}\cdot T^2 + 9.276772204\cdot10^{-9}\cdot T^3 - 3.588141876\cdot10^{-12}\cdot T^4$
		$879<T\leq1223$ K
		$n = 0.04628421012 + 0.000197951907\cdot T - 3.314868215\cdot10^{-7}\cdot T^2 + 1.3913294\cdot10^{-10}\cdot T^3$
Strain rate sensitivity exponent (unitless)	$293<T\leq752.5$ K	
	$m = 0.02280034483 - 3.448275862\cdot10^{-7}\cdot T$	
	$752.5<T\leq902.1$ K	
	$m = -2.534966886 + 0.006626767224\cdot T - 5.303091629\cdot10^{-6}\cdot T^2 + 1.34653092\cdot10^{-9}\cdot T^3$	
	$902.1<T\leq1223$ K	
	$m = -0.1619955889 + 3.080302048\cdot10^{-4}\cdot T$	

Table 6. Anisotropy coefficients F, G, H versus temperature and cladding type.

Coefficient	Cladding type	
	Unirradiated	Irradiated
F (unitless)	$293<T\leq1273$ K	$293<T\leq515.9$ K
	$F= 1.39239 - 4.63177\cdot10^{-3}\cdot T+ 1.62105\cdot10^{-5}\cdot T^2 - 2.58537\cdot10^{-8}\cdot T^3 + 1.8076\cdot10^{-11}\cdot T^4 - 4.60713\cdot10^{-15}\cdot T^5$	$F= 4.82048 - 4.21033\cdot10^{-2}\cdot T + 1.618275\cdot10^{-4}\cdot T^2 - 2.68661\cdot10^{-7}\cdot T^3 + 1.60548\cdot10^{-10}\cdot T^4$
	$T>1273$ K	$515.9<T\leq823$ K
	$F=0.5$	$F= 20.522409 - 1.14701\cdot10^{-1}\cdot T + 2.46179\cdot10^{-4}\cdot T^2 - 2.33290\cdot10^{-7}\cdot T^3 + 8.21321\cdot10^{-11}\cdot T^4$
		$T>823$ K
		$F=0.5$
G (unitless)	$293<T\leq1273$ K	$293<T\leq560$ K
	$G=-6.6085\cdot10^{-2} + 4.28093\cdot10^{-3}\cdot T^2 - 1.51357\cdot10^{-5}\cdot T^2 + 2.41818\cdot10^{-8}\cdot T^3 - 1.72441\cdot10^{-11}\cdot T^4 + 4.49996\cdot10^{-15}\cdot T^5$	$G= 1.39276 - 1.792591\cdot10^{-2}\cdot T + 1.19333\cdot10^{-4}\cdot T^2 - 3.776742\cdot10^{-7}\cdot T^3 + 5.69241\cdot10^{-10}\cdot T^4 - 3.247347\cdot10^{-13}\cdot T^5$
	$T>1273$ K	$560<T\leq823$ K
	$G=0.5$	$G= -1.541960 + 8.715936\cdot10^{-3}\cdot T - 1.17013\cdot10^{-5}\cdot T^2 + 5.010771\cdot10^{-9}\cdot T^3$
		$T>823$ K
		$G=0.5$

Coefficient	Cladding type	
	Unirradiated	Irradiated
H (unitless)	$293<T\leq1273$ K	$293<T\leq823$ K
	$H = 0.173693 + 3.50846\cdot10^{-4}\cdot T - 1.074777\cdot10^{-6}\cdot T^2 + 1.67189\cdot10^{-9}\cdot T^3 - 8.31926\cdot10^{-13}\cdot T^4 + 1.07169\cdot10^{-16}\cdot T^5$	$H = 0.5178583 - 1.71631\cdot10^{-3}\cdot T + 5.313208\cdot10^{-6}\cdot T^2 - 7.13646\cdot10^{-9}\cdot T^3 + 3.870678\cdot10^{-12}\cdot T^4$
	$T>1273$ K	$T>823$ K
	H=0.5	H=0.5

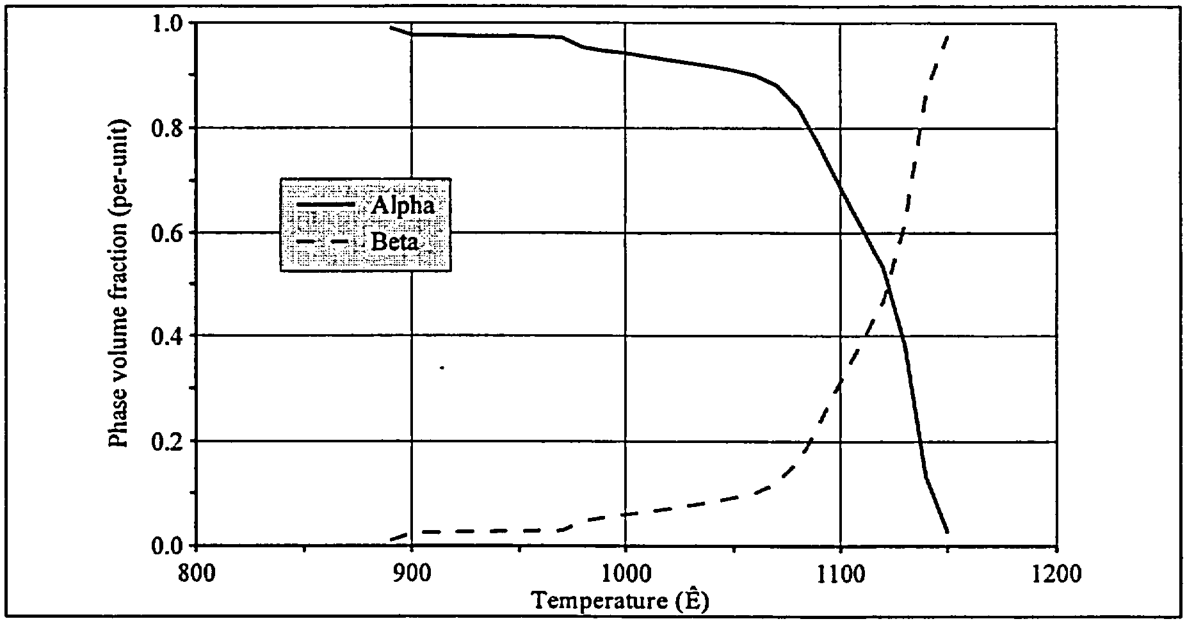

Fig. 1. Volumetric fractions of α and β-phases depending on Zr-1%Nb alloy temperature [18].

2.3. High temperature oxidation kinetics

In the FRAPTRAN code, high temperature Zry cladding oxidation calculations were provided for using two models selected by the user:

1. Baker-Just model [20];
2. Cathcart-Pawel model [21].

At that, Baker-Just model is used as the conservative oxidation kinetics, and Cathcart-Pawel model – as the best estimate model.

The same way as for the Zry cladding, two high temperature oxidation models for Zr-1%Nb cladding can be suggested. Thus, the conservative kinetics used in Russia for licensed calculations of VVER fuel rods [22] was implemented in the MATPRO package. The corresponding analytical correlations for weight gain, ZrO_2 and $\alpha Zr(O)$ layer thicknesses are given in Table 7.

As to the best estimate model, the authors of this report currently recommend using the existing Cathcart-Pawel model as such a model for Zr-1%Nb cladding. This model describes the last test data obtained at NSI

RRC KI and RIAR the most closely (see Fig. 2). At that, developing of the separate best estimate kinetics for E110 is found to be premature for the time being due to incompleteness of the experimental program, the results of which will be published in 2002 in another NSI/IRSN/NUREG report.

Table 7. Conservative oxidation kinetics for Zr-1%Nb cladding.

Oxidation parameter	Nomenclature	Temperature range	Routine
$\Delta m=9.2\cdot10^{2}\exp(-10410/T)\sqrt{\tau}$	Δm – weight gain [mg/cm^2]		COXTHK
$\delta_{ZrO2}=1.04\exp(-12240/T)\sqrt{\tau}$	δ_{ZrO2} – ZrO_2 oxide layer [cm]		COXWTK
$\delta_{Zr(O)}=5.68\cdot10^{-2}\exp(-6790/T)\sqrt{\tau}$	$\delta_{Zr(O)}$ – α-Zr(O) layer [cm]	1173<T<1773K	
	τ- time (s);		
	T – temperature (K);		

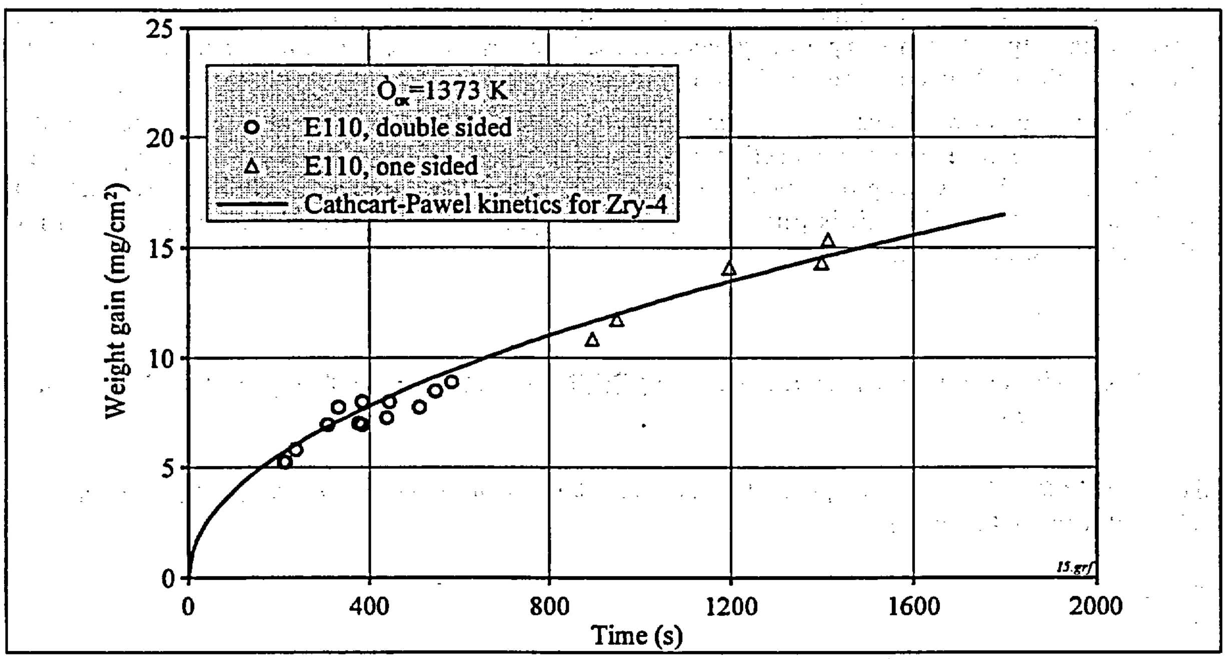

Fig. 2. Comparison of test data on Zr-1%Nb steam oxidation with Cathcart-Pawel model predictions.

3. FRAPTRAN MODIFICATIONS FOR VVER FUEL ROD SIMULATION

This section gives a description of modifications made to the original version of FRAPTRAN. As was already noted, in addition to incorporating alternative cladding material properties, certain modifications of models and algorithms were necessary in order for the code to be able to correctly simulate VVER fuel rod behavior. Mainly, the modifications were imposed by the following characteristics of the fuel geometry and conditions of tests, which were selected as the assessment cases:

- presence of a central hole in the fuel pellet. This condition had to be taken into consideration in calculating of volumetric heat generation rate, normalized radial power profile, and fuel radial displacement;
- carrying out of power pulse tests of single rods in ampoule conditions (large volume of stagnant water under normal conditions). These test rod cooling conditions cannot be quite adequately described by the heat transfer models that exist in the original version of FRAPTRAN. Therefore, alternative models for film boiling and rewetting models were needed;
- absence of strain component in the cladding mechanical model due to high temperature creep. Neglecting creep during certain stages of LOCA when stresses in the cladding may not reach the yield point and/or may decrease with time may result in erroneous predictions of deformation and rupture in cases when only instantaneous plasticity model is used. That is why incorporating the creep components into mechanical calculations was considered an important task;
- significant scope of modifications in the material property models and in the calculation modules of the body text of the code caused introduction of a large number of global and local variables, input/output variables, as well as writing of a number of new subroutines. Therefore, this section gives a detailed explanation of the modifications pertaining to coding aspects. This might prove to be useful both for developers and users of the code.

3.1. Volumetric heat generation rate (HGR) calculation for fuel pellet with central hole

In the original FRAPTRAN version, radially averaged volumetric heat generation rate is calculated only for a fuel pellet without the central hole:

$$q_v = \frac{q_l}{\pi r_{fo}^2},$$

where q_v – radially averaged volumetric HGR (W/m^3);

q_l – radially averaged linear HGR (W/m);

r_{fo} – fuel outer radius (m).

In this work, the determination of the radially averaged volumetric heat generation rate in the case of VVER-type fuel pellets with central hole was modified as:

$$q_v = \frac{q_l}{\pi(r_{fo}^2 - r_{fi}^2)},$$

where r_{fi} – fuel inner radius (m).

3.2. Radial power profile calculation for fuel pellet with central hole

Initially, radial power distribution is determined for a fuel pellet without central hole with the following normalization:

$$\frac{\int_0^{r_{fo}} K_r dr}{\pi r_{fo}^2} = 1,$$

where $K_r = \frac{q_l(r)}{\bar{q}_l}$ – normalized radial power factor (unitless);

$q_l(r)$ – linear HGR at current fuel radius (W/m);

$\bar{q}_l$ – radially averaged linear HGR (W/m).

The condition for normalized radial power factor in the case of VVER-type fuel pellets with central hole is introduced in the following form:

$$\frac{\int_{r_{fi}}^{r_{fo}} K_r dr}{\pi (r_{fo}^2 - r_{fi}^2)} = 1.$$

3.3. Calculation of the radial displacement of fuel due to thermal expansion for pellet with central hole

The radial displacement of the fuel pellet due to thermal expansion was modified for the case of fuel with central hole in the following manner:

$$U_T = \int_{r_{fi}}^{r_{fo}} \varepsilon(T) dr,$$

where U_T – fuel radial displacement (m);

$\varepsilon(T)$ – fuel thermal expansion (m/m);

r_{fo} – fuel outer radius (m);

r_{fi} – fuel inner radius (m).

Additional term U_c of the pellet radial displacement named as "hour-glassing" effect is calculated using the expression:

$U_c = 0.0025 r_{fo}$,

$U_c = 0.0025 r_{fo}(1-P/34.5)$, if $0<P<34.5$,

$U_c = 0$, if $P \geq 34.5$,

where P – fuel/cladding contact pressure (MPa).

Besides, the fuel relocation term U_{rel} is accounted for in the fuel radial displacement:

$U_{rel} = 0.3\Delta_{gap}$ – for fresh fuel,

$U_{rel} = 0.45\Delta_{gap}$ – for high-burnup fuel,

where Δ_{gap} – initial gap width.

At the current stage of the code assessment, the following effects of the pellet radial displacement were eliminated for VVER-type fuel pellets:

- Fuel expansion due to "hour-glassing" effect;
- Fuel relocation at the beginning of a pulse test (U_{rel}=0).

3.4. Alternative Post-Critical Heat Flux heat transfer model

The model for post-critical heat transfer coefficient (HTC) calculations based on Bromley-Pomerantz correlation [23] was replaced with the Labuntzov model. This model was developed for the turbulent regimes of film boiling and was modified to account for the boiling conditions of the large volume of subcooled water [24]:

$$\alpha_{FB} = 0.25(\lambda_g^2 c_{pg}(\rho_f - \rho_g)\frac{g}{v_g})^{1/3},$$

where α_{FB} – heat transfer coefficient (W/m^2K);

λ_g – vapor thermal conductivity (W/m K);

c_{pg} – vapor specific heat (J/kg K);

ρ_f – fluid density (kg/m^3);

ρ_g – vapor density (kg/m^3);

g – Gravity acceleration (m/s^2);

v_g – vapor kinematic viscosity (m^2/s).

To take into account the initial subcooling of water, the correction factor is introduced [25]:

$$\alpha_{FB}^{\bullet} = \alpha_{FB}(1 + 0.1(\frac{\rho_f}{\rho_g})^{0.75}\frac{\Delta i}{h_{fg}}),$$

where $\alpha^{\bullet}_{FB}$ – corrected heat transfer coefficient (W/m^2 K);

Δi – enthalpy of fluid at saturation minus enthalpy at fluid bulk temperature (J/kg).

Thermal-physical properties of vapor are determined at film temperature:

$$T_{film} = \frac{T_{wall} + T_s}{2},$$

where T_{wall} – cladding temperature (K);

T_s – saturation temperature (K).

3.5. Cladding rewetting model for IGR/RIA tests

The moment when rewetting begins is determined with the model developed by RRC KI [3, 26]. Rewetting moment calculation option is specified in the input data. Heat transfer coefficient in the transition mode from film boiling to nucleate boiling in determined by means of linear interpolating between two points on the boiling curve. The first point corresponds to the film boiling heat transfer coefficient at the moment when rewetting begins. The second point corresponds to the heat transfer coefficient in the case of complete wetting, i.e. at nucleate boiling, and is determined per critical heat flux of the second type. 2-D heat conduction equation with quench front movement boundary condition is resolved analytically:

$$C_p \rho \frac{\partial T}{\partial \tau} = \frac{\partial}{\partial z}\left(\lambda \frac{\partial T}{\partial z}\right) + \frac{1}{r}\frac{\partial}{\partial r}\left(\lambda r \frac{\partial T}{\partial r}\right) + q_v,$$

where C_p – specific heat capacity;

T – temperature (r, z, τ);

λ – clad heat conductivity;

q_v – volumetric internal heat source;

ρ – clad density.

Obtained approximate analytical solution for quench front velocity and time of rewetting is expressed by the following equation:

$$z(t)=\int_{t_0}^{t_w} u(t)dt,$$

where t – time;

z – axial coordinate;

U(t) – quench front movement rate;

t_0 – time when transition boiling begins (Tclad=640 K);

t_w – rewetting time.

Currently the rewetting model does not implenented into FRAPTRAN code. The time of rewetting is specified on the base of previous FRAP-T6 (modified) calculations.

3.6. Zr-1%Nb high temperature creep model for MATPRO and SCANAIR

In the FRAPTRAN code, cladding stress-strain equations include components of thermal, elastic and plastic deformation [11].

Description of the fuel rod deformation under the loss-of-coolant accident conditions, as compared to the reactivity increase accident conditions, has a number of peculiarities, the most important of which is that, in a number of LOCA scenarios, the duration of the high temperature cladding deformation process is on the order of hundreds of seconds. Besides, cladding deformation over a significant period of time can occur under the mechanical loading conditions when stresses in the cladding do not exceed the material yield stress, or at monotonous mechanical load dropping. Therefore, it is proposed to modify cladding mechanical behavior equations using material visco-plastic deformation model.

Modification of the cladding stress-strain equations consists in that elastic and plastic deformation equation components are supplemented with viscous deformation components.

Thus, the cladding mechanical model in the FRAPTRAN (modified) code includes description of cladding thermal expansion effects, elastoplastic deformation effects and cladding material high temperature creep effects. Additivity assumption for thermal, elastic, plastic and viscous strains is used. In order to describe cladding mechanical state, Hooke's law and Prandtl-Reuss visco-plastic flow model that can be written down in strain increments as shown below are used:

$$\varepsilon_\theta=\frac{1}{E}\{\sigma_\theta-\nu\sigma_z\}+\varepsilon_\theta^p+d\varepsilon_\theta^p+\varepsilon_\theta^c+d\varepsilon_\theta^c+\int_{T_0}^{T}\alpha dT \quad (1)$$

$$\varepsilon_z=\frac{1}{E}\{\sigma_z-\nu\sigma_\theta\}+\varepsilon_z^p+d\varepsilon_z^p+\varepsilon_z^c+d\varepsilon_z^c+\int_{T_0}^{T}\alpha dT \quad (2)$$

$$\varepsilon_r=-\frac{\nu}{E}\{\sigma_\theta-\sigma_z\}+\varepsilon_r^p+d\varepsilon_r^p+\varepsilon_r^c+d\varepsilon_r^c+\int_{T_0}^{T}\alpha dT \quad (3)$$

where T_0 – initial cladding temperature;

T – current cladding temperature;

α – temperature expansion factor;

E – modulus of elasticity;

ν – Poisson's ratio;

ε_θ, ε_z, ε_r – full cladding deformation in hoop, axial and radial directions;

$\varepsilon_\theta^P, \varepsilon_z^P, \varepsilon_r^P$ – plastic cladding deformation in hoop, axial and radial directions;

$d\varepsilon_\theta^P, d\varepsilon_z^P, d\varepsilon_r^P$ – plastic cladding deformation in hoop, axial and radial directions at time increment dt;

$\varepsilon_\theta^C, \varepsilon_z^C, \varepsilon_r^C$ – viscous cladding deformation in hoop, axial and radial directions;

$d\varepsilon_\theta^C, d\varepsilon_z^C, d\varepsilon_r^C$ – viscous cladding deformation in hoop, axial and radial directions at time increment dt;

$\sigma_r, \sigma_\theta, \sigma_z$ – radial, hoop and axial stress components, respectively.

At each time increment, plastic and viscous strain increments ($d\varepsilon^P$ and $d\varepsilon^C$) are determined in accordance with the Prandtl-Reuss flow rule.

Increments of the plastic strain components are determined per effective stress σ_e and effective plastic strain according to the stress-strain diagram. Creep strain component increments – per effective stress and average cladding temperature in accordance with experimentally obtained dependence for material creep rate given in Tablè 4 of Section 2.2.

Modified technique for fuel rod cladding deformation behavior calculation is implemented in CLADF and BALON2 subroutines. Block diagram for calculating of cladding mechanical response using the modified model in FRAPTRAN code is shown in Fig. 3.

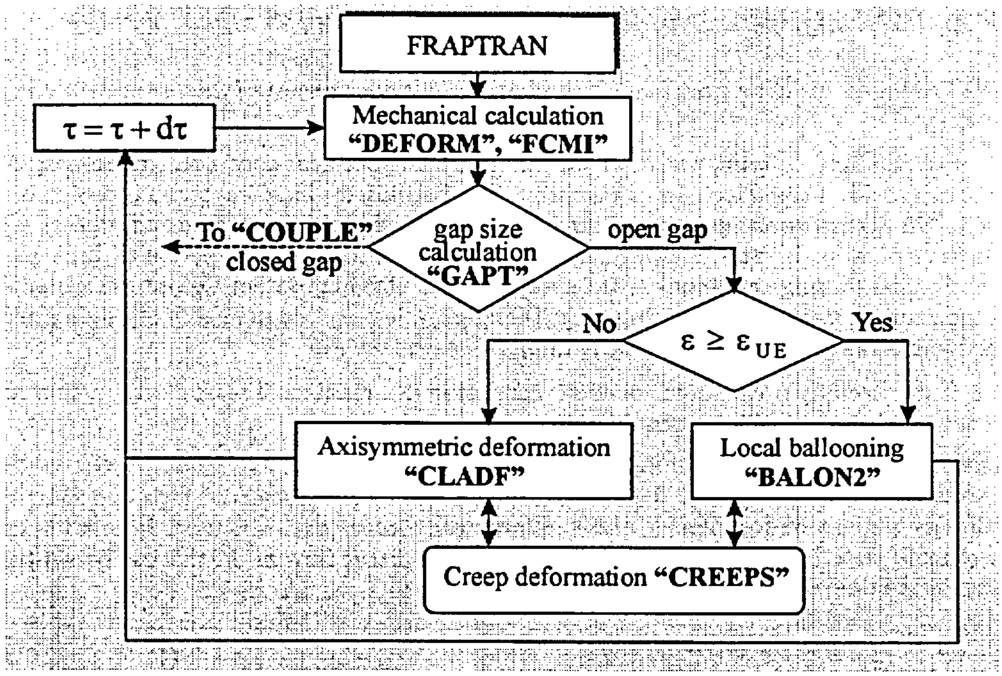

Fig. 3. Block diagram for calculating of cladding mechanical response using modified model in FRAPTRAN code (modified).

3.7. Description of modified routines and coding aspects

3.7.1. Description of the new global variables

The new global variables are introduced for the newly developed and modified models. Table 8 contains the description of the new global variables. All new global variables stored in WWER.H* header. Currently IWWER indicator is temporarily used to recognize the cladding type. In the near future, ICM indicator with option of ICM=6 for Zr-1%Nb cladding type will be introduced in FRAPTRAN and MATPRO subroutines instead of IWWER indicator.

Table 8. New global variables incorporated into FRAPTRAN code.

Name	Type	Storage	Description
iwwer	INTEGER*8	wwer.h common /wwer/	Option for selection of Zr-1%Nb cladding type
nfilm	INTEGER*8	wwer.h common /wwer/	Indicator for Labuntzov or Bromley-Pomerantz models used for film boiling heat transfer calculation
icreep	INTEGER*8	wwer.h common /wwer/	Indicator to use the cladding creep model: 0 – the model is not used 1 – creep model is used
jzmax	INTEGER*8	wwer.h common /wwer/	Axial slice number for printout of time dependent fuel rod parameters
rfi	REAL*8	wwer.h common /mech/	Radius of central hole in pellets. rfi is used in HEAT and POWER routines to correctly compute volumetric heat generation rate in fuel pellet with central hole
irr	REAL*8	wwer.h common /wwer/	Indicator for selection of Zr-1%Nb cladding mechanical properties: 0 – unirradiated cladding properties 1 – irradiated cladding properties
moxid	REAL*8	cobild.f	Indicator to select the model for high-temperature oxidation of Zr-1%Nb cladding: 5 - conservative model

3.7.2. Description of the new and modified subroutines

Table 9 lists the modified subroutines of FRAPTRAN code and presents description of the new and modified subroutines.

Table 9. List of modified routines of FRAPTRAN code.

Routine	Function	Modification or implementation
Implementation of Zr-1%Nb material properties into MATPRO original subroutines		
CCP	Function for calculation of clad specific heat	Zr-1%Nb clad specific heat.
CCPINP	Driver for calculation of clad enthalpy	Zr-1%Nb clad enthalpy.
CTHEXP	Driver for calculation of clad thermal expansion	Zr-1%Nb clad thermal expansion.
CELMOD	Driver for calculation of clad Young's modulus	Zr-1%Nb clad Young's modulus.
CSHEAR	Function for calculation of clad shear modulus	Zr-1%Nb clad shear modulus.

* Although the name of the header "WWER" is rather arbitrary, in order to avoid contradictions it needs to be said that in literature one may find double spelling of the abbreviation for the Russian pressurized water reactor – VVER and WWER.

Routine	Function	Modification or implementation
CTHCON	Driver for calculation of clad thermal conductivity	Zr-1%Nb clad thermal conductivity.
CMHARD	Function for calculation of clad Mayer micro-hardness	Zr-1%Nb clad Mayer micro-hardness.
CKMN	Driver for calculation of K, m, n clad parameters for clad plastic stress-strain curve	Calculation of Zr-1%Nb K, m, n clad parameters for fresh and irradiated type of cladding.
CMLIMT	Driver for calculation of clad short-term strength and plastic parameters	Calculation of Zr-1%Nb clad ultimate strength parameters for cladding failure evaluation.
CANISO	Routine for calculation of cladding anisotropy coefficients. CANISO is not used in mechanical calculation	Calculation of anisotropy coefficients F, G, H for fresh and irradiated type of Zr-1%Nb cladding.
COBILD	Driver for calculation of high-temperature oxidation	Calculation of weight gain, ECR, Zr- and Zr(O)-oxide layers for Zr-1%Nb clad. Driver calls COXTHK and COWTK subroutines.
PHYPRP	Driver for calculation of fuel and cladding thermal-physical parameters	Introduction of thermal-physical parameters for Zr-1%Nb clad (fusion heat, alpha- and beta-phase temperatures, melt point etc.).
	New models and subroutines	
QDOT	Driver for calculation of clad-to-coolant heat transfer coefficients	Calculation of clad-to-water heat transfer coefficient was developed for the turbulent regimes of film boiling and modified to account for the boiling conditions of the large volume of subcooled water (Labuntzov model). Input parameter nfilm is used as optional variable
CREEPS	New subroutine for clad creep rate calculation under high-temperature conditions	Computation of creep rate of Zr-1%Nb cladding versus temperature and effective stress. Subroutine was coded for the MATPRO package
COXTHK	New subroutine adopted from MATPRO/ RELAP5 [27] and supplied with the Zr-1%Nb growth rate constant for oxide thickness, oxygen-stabilized alpha layer thickness, and thickness of the beta layer	COXTHK and COXWTK subroutines contain conservative model (moxid=5) of high-temperature oxidation for Zr-1%Nb. moxid – optional variable for oxidation models
COXWTK	New subroutine adopted from MATPRO/ RELAP5 [27] and supplied with the growth rate constant for weight gain for Zr-1%Nb cladding	
	Modifications and corrections	
PRNTOT	Print output information in listing	1. Implementation of the additional output parameters to listing and time dependent parameters for secondary plot file 'FORT.DAT' 2. Correction of the average fuel temperature calculation accounting for a central hole in the fuel pellet
FRAPTRAN	Major driver. Routine reads control variables	Reading new input variables for VVER conditions (iwwer, nfilm) and a fuel rod slice number to plot (jzmax)
	To account for user-specified fission gas release in calculation relfrac input array is determined as: relfrac(mfgr) mfgr=25 User-specified array of fuel displacement due to fuel gas swelling is determined as time-dependent displacement table: FuelGasSwell(mfs) mfs=25	Elimination of the mistake associated with dimensions of relfrac and FuelGasSwell arrays. To correct reading of the time dependent tables of fission gas release and transient fuel swelling, the dimensions of relfrac and FuelGasSwell arrays were set as: mfgr=50 mfs=50 Thus, all 25 pairs of points can be read from input deck.
IOFILES	Driver reads input data in NAMELIST format and clad nodalization setup. Default value of clad mesh points ncmesh=2	Extension of clad nodalization by implementation of integer variable ncmesh and cmesh array for clad radial coordinates into NAMELIST: namelist /solution/ dtmaxa, dtss, prsacc, tmpac1, soltyp, maxit, noiter, epsht1, naxn, zelev, nfmesh, fmesh, ncmesh, cmesh

Routine	Function	Modification or implementation
COMINP	Recalculation and processing input parameters of fuel rod. Integration of radial power profile in fuel	Correction of calculation of radial power profile integral in fuel pellet with central hole
INITIA	Initialization of all variables in transient calculations. Integration of radial power profile in fuel	The same problem as in COMINP
	Calculation of fission gas inventory in high-burnup fuel. Fuel volume is calculated only for fuel without central hole	Introduction of fuel volume calculation for pellets with central hole to obtain generated fission gas products
COUPLE	Mechanical calculation of fuel-cladding interaction. Clad temperature limit (tedot=1089 K), at which the cladding strain rate becomes excessive, is set. In this case calculation continues bypassing the normal iterative solution	For Zr-1%Nb cladding clad temperature limit equal to 1030 K was obtained. tedot=1030 K This limit was obtained during checking of the code working with Zr-1%Nb mechanical property correlations
CMLIMT	FRAPTRAN uniform cladding strain for Zry cladding was adopted from FRAPCON-3 code [28]: $e_u = 0.096 - 1.142 \cdot 10^{4} T +$ $0.01856 \exp(-F/10^{25}) - \sqrt{\dfrac{h_{ex}}{8.05 \cdot 10^{5}}}$ T-temperature (K); F - fast fluence (n/m^2); h_{ex} – excess hydrogen concentration (ppm)	Elimination of uniform cladding strain for Zry adopted from FRAPCON-3 code. Because this correlation is valid only in low-temperature range between 580 and 680 K. Under temperatures more than 840 K uniform strain becomes negative. So, the dependence of uniform strain is described by FRAP-T6 (V21) relationship both for Zry and Zr-1%Nb cladding: $e_u = \exp(\dfrac{n}{1+m}) - 1$ n – strain hardening exponent (unitless); m – strain rate sensitivity exponent (unitless)
POWER	Subroutine specifies fuel rod power as function of time and axial elevation. Determination of volumetric heat generation rate (HGR) in fuel in following form: $q_v = \dfrac{q_l}{\pi r_{fo}^2}$, q_v – volumetric HGR (W/m^3); q_l – linear HGR (W/m); r_{fo} – fuel outer radius (m)	Correction of the way volumetric heat generation rate is determined for fuel with central hole. So, For the fuel without hole $q_v = \dfrac{q_l}{\pi r_{fo}^2}$ For the fuel with hole $q_v = \dfrac{q_l}{\pi (r_{fo}^2 - r_{fi}^2)}$ r_{fi} – fuel inner radius (m)
COMPUT	Driver for global computation of the fuel rod variables vs. time. Routine calls COBILD, where clad linear power due to oxidation reaction is computed by equation: $P = 1.15\ 10^8\ \Delta w\ D_{fr}/(2\ dt)$, P – linear power (W/m); Δw - weight gain (kg/m^2); D_{fr} – fuel rod outer diameter (m); dt – time increment (s) Clad temperature limit for beginning of high-temperature oxidation (tempc1) is equal to 1073 K	1. Correction of average fuel temperature calculation in fuel pellet accounting for central hole (the same correction as in PRNTOT routine). 2. Elimination of clad temperature limit for beginning of high-temperature oxidation (tempc1>1073 K). Time increment less than 0.001s leads to prompt increase of clad linear power (at the first time increment) and the clad temperature above the limit of 1073 K. This results in local increase of outer clad temperature. So, the elimination of temperature threshold provides for the continuity of linear power function vs. clad temperature.

Routine	Function	Modification or implementation
	In COMPUT routine, determination of the current value of transient fuel swelling is done by interpolation: TranFuelSwell = POLATE(FuelGasSwell,Time,50,iu) where: 'FuelGasSwell' – time dependent input fuel swelling table 'Time' – current time	Correction of wrong entry to POLATE function: TranFuelSwell = POLATE(FuelGasSwell,Time,25,iu) 25 – number of pairs of entries in 'FuelGasSwell' array
DEFORM	Computation of the deformed fuel radius due to transient fuel swelling: $R_f = R_{def} \cdot TranFuelSwell$ R_f – fuel radius (m); R_{def} – deformed fuel radius due to thermal expansion, relocation and steady-state swelling (m); TranFuelSwell – relative change in deformed fuel radius (R_{def}) due to transient fuel swelling (1.0 - no fuel swelling) (unitless)	Modification of the approach to determine deformed fuel radius due to transient fuel swelling: $R_f = R_{def} + R_{cold} \cdot (TranFuelSwell-1)$ R_{cold} – cold fuel radius (m); TranFuelSwell - relative change in cold fuel radius (R_{cold}) due to transient fuel swelling (unitless). This approach is more suitable for specifying deformation history of fuel radius based on the net transient fuel swelling
Routines: IOFILES CARDIN POWER FCMI2 Headers: BCDCOM POWRD	IOFILES subroutine controls the input data and specifies the array for average linear heat generation rate: nptha1=200 RodAvePower(nptha1,100) That is the 'RodAvePower' array that contains 100 pairs of time-power points	Extension of 'RodAvePower' array for average linear heat generation rate from 100 points to 1000: nptha1=2000 RodAvePower (nptha1,100) Thus, 'RodAvePower' array contains 1000 pairs of time-power points

3.7.3. Description of the new input variables

Temporarily the additional parameters occupy three first strings in the input deck specification. Description of the new input parameters is presented in Table 10.

Table 10. List of new input data parameters.

Parameter	Description	Type	Value
iwwer	VVER/PWR type of cladding • Cladding – Zircaloy • Cladding - Zr-1%Nb	INTEGER*8	 0 1, 2*
nfilm	Indicator of the film boiling HTC • Bromley-Pomerantz model • Labuntzov model	INTEGER*8	 0 1
icreep	Indicator to use cladding creep model • Cladding creep model isn't used • Cladding creep model is used	INTEGER*8	 0 1
jzmax	Axial fuel rod slice number for the secondary plot file 'FORT.DAT'	INTEGER*8	1-kmax

* IWWER=1 implies using heat capacity of Zr-1%Nb obtained for low heatup rates, whereas under IWWER=2 heat capacity for high heatup rates (1000 K/s) is used. Other thermal and mechanical properties are identical.

3.7.4. Description of additional output information

Generating of the following files is provided for in order to depict information on cladding residual strain caused by high temperature creep (Table 11).

Table 11. Output information files.

Filename	Output information parameter	Variable name	Format
CREEPH.DAT	Cladding creep hoop strain	creeph	REAL*8 array(50)
CREEPZ.DAT	Cladding creep axial deformation	creepz	REAL*8 array(50)
CREEPR.DAT	Cladding creep radial deformation	creepr	REAL*8 array(50)
ERESH.DAT	Total cladding creep and plasticity hoop strain Relative contribution of plasticity and creep deformation into the overall deformation (for the maximum stress cross-section)	eresh, splast, screep	REAL*8 array(50) REAL*8 constant REAL*8 constant
ERESZ.DAT	Total cladding creep and plasticity axial deformation	eresz	REAL*8 array(50)
ERESR.DAT	Total cladding creep and plasticity radial deformation	eresr	REAL*8 array(50)

Cladding strain is recorded in the output files depending on time for each axial segment of the cladding. Description of additional parameters in output data files is provided in Table 12.

Table 12. Additional parameters in output data files.

Variable name	Parameter	Unit of measurement
t_s	Time	s
creeph(j*)	Cladding creep hoop strain	%
creezh(j)	Cladding creep axial deformation	%
creerh(j)	Cladding creep radial deformation	%
eresh(j)	Total cladding creep and plasticity hoop strain	%
splast(jzmax**)	Relative contribution of plasticity deformation into the overall deformation	%
screep(jzmax)	Relative contribution of creep deformation into the overall deformation	%
eresz(j)	Total cladding creep and plasticity axial deformation	%
eresr(j)	Total cladding creep and plasticity radial deformation	%

4. CODE ASSESSMENT AGAINST IN-PILE IGR/RIA AND OUT-OF-PILE RIAR/LOCA TEST DATA

The most general principles that called forth the test case selection for the present work are illustrated in Table 13. There is an assessment matrix of fuel rods tested in IGR reactor under RIA conditions and in RIAR out-of-pile LOCA test facility presented there.

Three assessment cases were selected to simulate fresh fuel rod behavior (instrumented test rods 50F-13, 50F-16, 96F-09). Test results were compared with calculation data obtained with of FRAPTRAN (original version), FRAPTRAN (modified), FRAPT-T6 (modified) and SCANAIR (modified) codes. As is shown in Table 13, the assessment cases for fresh fuel rods present the range of cladding temperatures from 293 to 1840 K and characterize boiling curve from free convection heat transfer to film boiling.

Three assessment cases were chosen to simulate high-burnup fuel rod behavior (H5T, H7T and H1T). High burnup fuel rod modeling results (H5T, H7T and H1T) were obtained earlier using FRAPT-T6 (modified), SCANAIR (modified) codes and are given in work [3]. The calculation results obtained using FRAPTRAN (modified) were compared with the results obtained using FRAPT-T6 (modified), SCANAIR (modified) codes. The obtained discrepancies in the main fuel rod thermal mechanical parameters were analyzed, and possible reasons for the differences were discovered.

Table 13. Assessment matrix of fuel rods tested in IGR reactor under RIA conditions and RIAR out-of-pile LOCA tests.

Assessment case	Type of test	Peak fuel enthalpy [3] (cal/g)	Assessed physical phenomena	Assessed fuel rod parameters	Measured parameters or calculational results
50F-13	RIA with fresh fuel	69	Nucleate boiling	cladding temperature	Cladding temperature history
50F-16	RIA with fresh fuel	139	Nucleate boiling CHF Post-CHF heat transfer	cladding temperature	Cladding temperature history
96F-09	RIA with fresh fuel	315	Nucleate boiling CHF Post-CHF heat transfer	cladding temperature, internal gas pressure	Cladding temperature and internal pressure history
H5T	High burnup RIA test	176	Nucleate boiling, CHF, Post-CHF heat transfer	Fuel and cladding temperature, internal gas pressure, cladding stress and strain, gap width etc.	Comparison with FRAP-T6 (modified) and SCANAIR (modified) calculation data
H7T	High burnup RIA test	187			
H1T	High burnup RIA test	151			
RIAR-LOCA2	Out-of-pile LOCA test	-	Cladding deformation and cladding failure	cladding strain, time of failure	Comparison with test data on cladding strains and time of failure

In order to verify FRAPTRAN code under LOCA conditions, calculations of Zr-1%Nb cladding deformation behavior under varying cladding heating and cooling modes and pressure increase rate (RIAR-LOCA2) were conducted. To study fuel rod behavior during the first stage of LOCA, a special facility with direct electric heating of fuel rods [1] was built at RIAR. This facility allows to conduct testing of fuel rod simulators with aluminum oxide filler in argon environment under the conditions modeling the first stage of LOCA. More detailed description of the installation and test procedures is given in Section 4.2.1.

4.1. IGR/RIA assessment

Principal fuel rod design parameters and IGR test conditions are listed in Table 14. The very detailed description of test data on power pulses, energy depositions, temperatures, and internal gas pressure is published in [3]. It should be noted that all selected test cases have already been discussed in detail in [3, 6, 7], where verification procedures for modified FRAP-T6 and SCANAIR codes were described. Therefore, comparison of FRAPTRAN calculations was performed not only with test data, but also with results obtained using modified versions of FRAP-T6 and SCANAIR codes.

Table 14. Brief description of fuel rod design parameters and IGR test conditions.

Parameter	Units	Value
Fuel rod type:		VVER-1000
Cladding		Zr-1%Nb
Fuel		UO_2
Burnup of mother rod	MWd/kg U	0; ≈50
Gas composition:		He-100%
Coolant		H_2O
Power half pulse width	ms	700-900
Cladding outside diameter	mm	9.1
Radial gap thickness	mm	0.03-0.12
Fuel pellet outer diameter	mm	7.57
Fuel pellet inner diameter	mm	2.2
Fuel stack height	m	0.15
Rod internal pressure	MPa	1.7-2.3
Coolant pressure	MPa	0.1
Coolant temperature	K	293
Coolant velocity	m/s	0.

4.1.1. 50F-13 IGR assessment case

Comparison of the measured and calculated cladding temperature histories is shown in Fig. 4. Predictions of the cladding temperatures under nucleate boiling conditions demonstrate a satisfactory agreement with the test data.

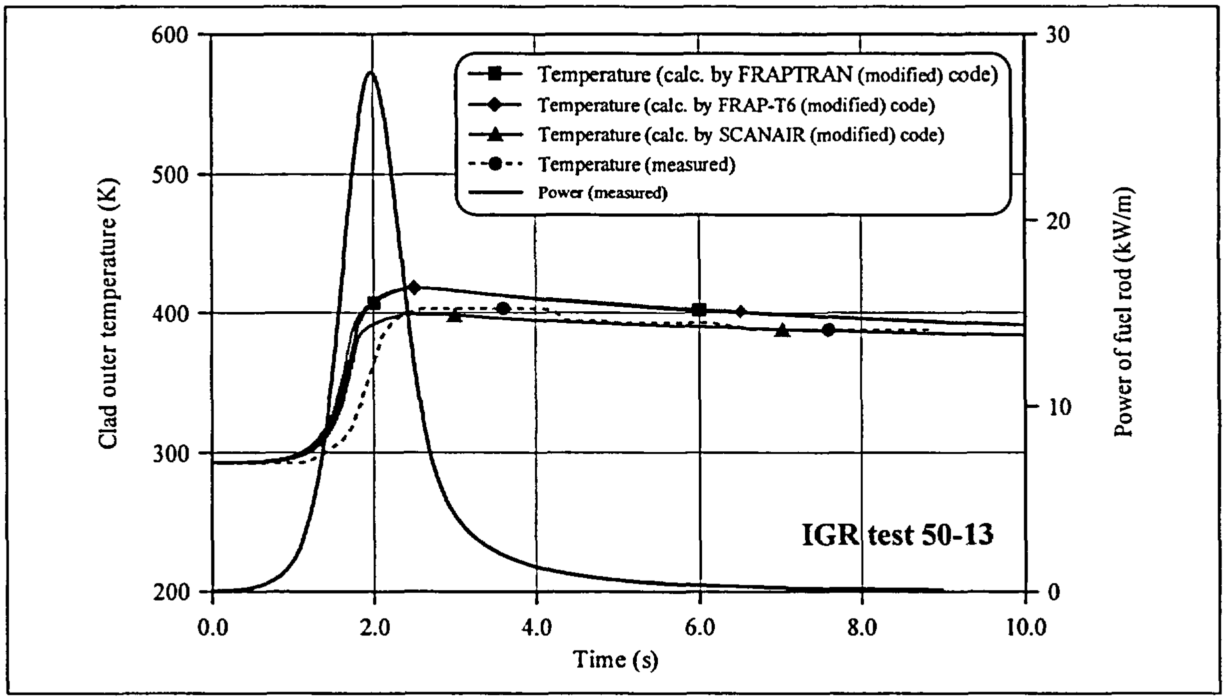

Fig. 4. Clad outer temperature in 50F-13 test: comparison between measured and calculated with FRAP-T6 (modified), SCANAIR (modified) and FRAPTRAN (modified) codes.

4.1.2. 50F-16 IGR assessment case

The cladding temperature history during IGR pulse test and calculated cladding temperature obtained with original version of the FRAPTRAN code are presented in Fig. 5. As shown in the plot, melting of cladding is predicted with original FRAPTRAN version.

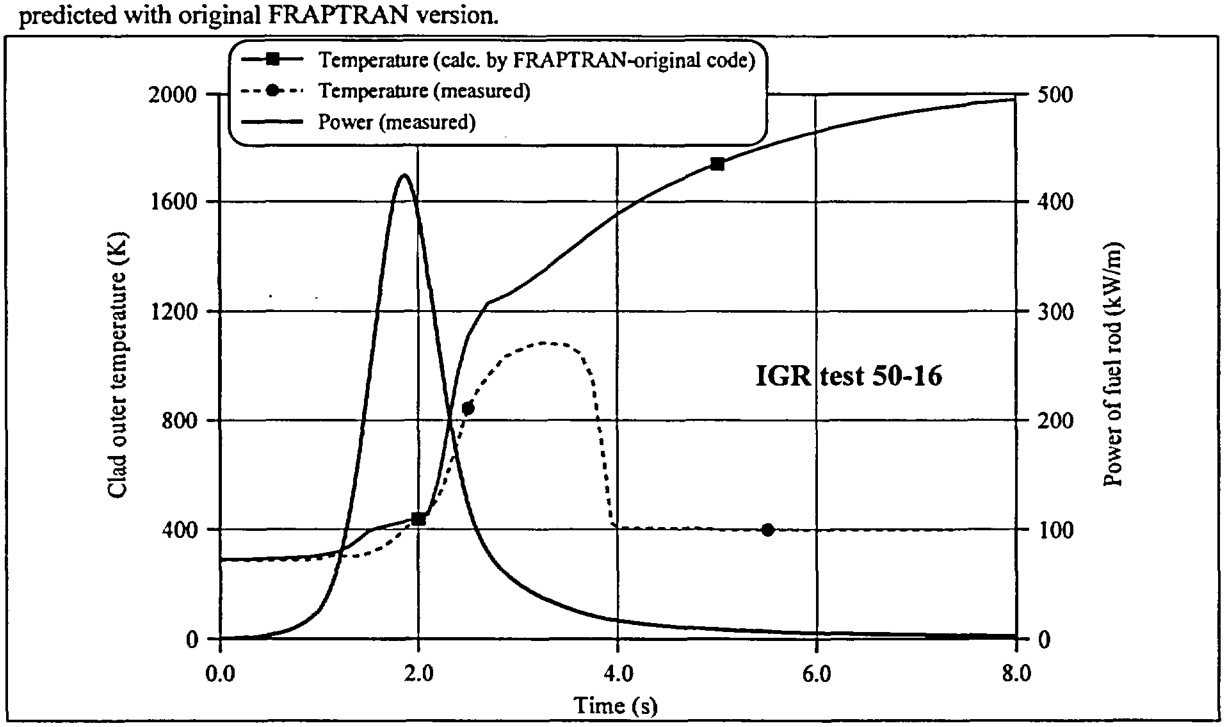

Fig. 5. Clad outer temperature in 50F-16 test: comparison between measured and calculated with original FRAPTRAN code.

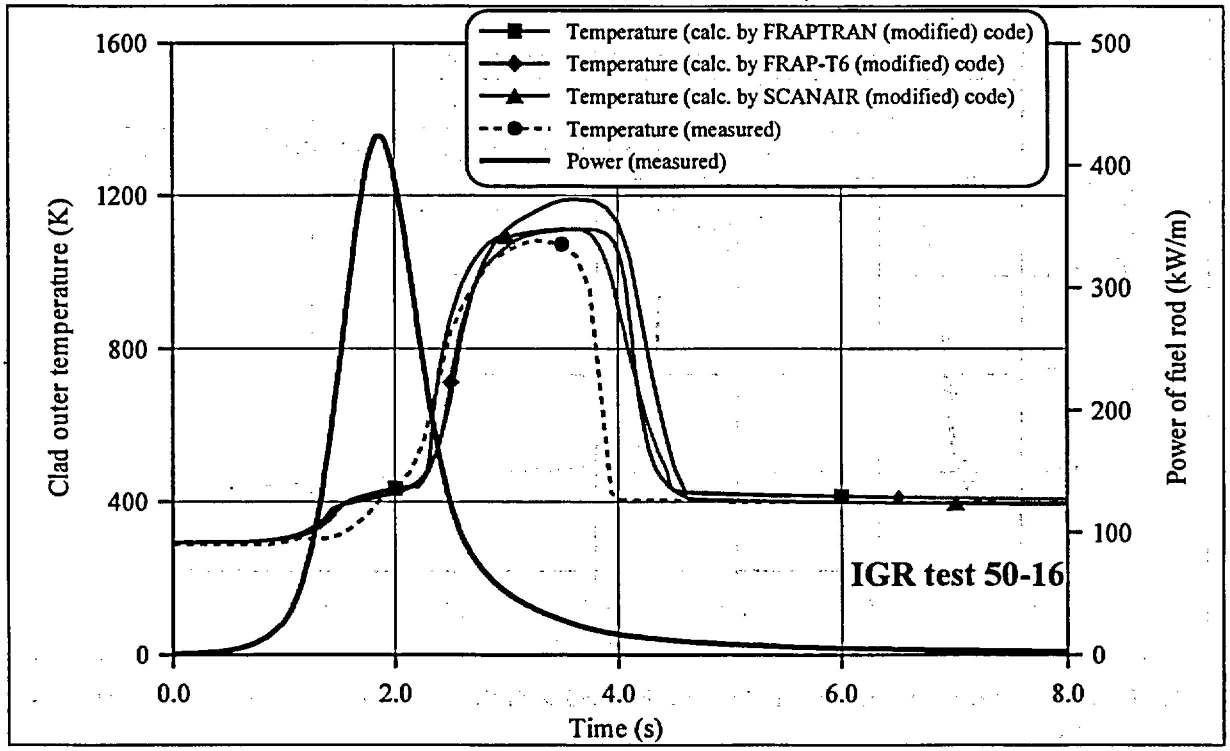

Fig. 6. Clad outer temperature in 50F-16 test: comparison between measured and calculated with FRAP-T6 (modified), SCANAIR (modified), and FRAPTRAN (modified) codes.

After the modifications of heat transfer model described in Section 3 of this report, the FRAPTRAN (modified) rather satisfactory predicts cladding temperature under nucleate boiling, transition boiling, and film boiling conditions (see Fig. 6).

4.1.3. 96F-09 IGR assessment case

Cladding temperature and internal gas pressure histories were measured during 96F-09 IGR pulse test [3]. These data and calculated results are shown in Fig. 7, Fig. 8, and Fig. 9. As the first step of assessment, the calculation with original version of FRAPTRAN was carried out. Cladding temperature history in this case is presented in Fig. 7. As shown in Fig. 7, cladding temperature rapidly achieved melting point due to insufficiently high clad-to-coolant heat transfer in post-CHF boiling regime.

Then the post-critical heat transfer calculation model based on Bromley-Pomerantz correlation was replaced with the Labuntzov model. After modification of the film boiling heat transfer coefficient, the next run was carried out with FRAPTRAN (modified). Thus, the comparison between measured cladding temperature and calculated data is presented in Fig. 8. Calculated cladding temperature was obtained previously with FRAP-T6 (modified). As shown in Fig. 8, the cladding temperature calculated with FRAPTRAN (modified) is in better agreement with experimental data than respective FRAP-T6 (modified) results. As shown in Fig. 9 the time of cladding failure is predicted accurately enough.

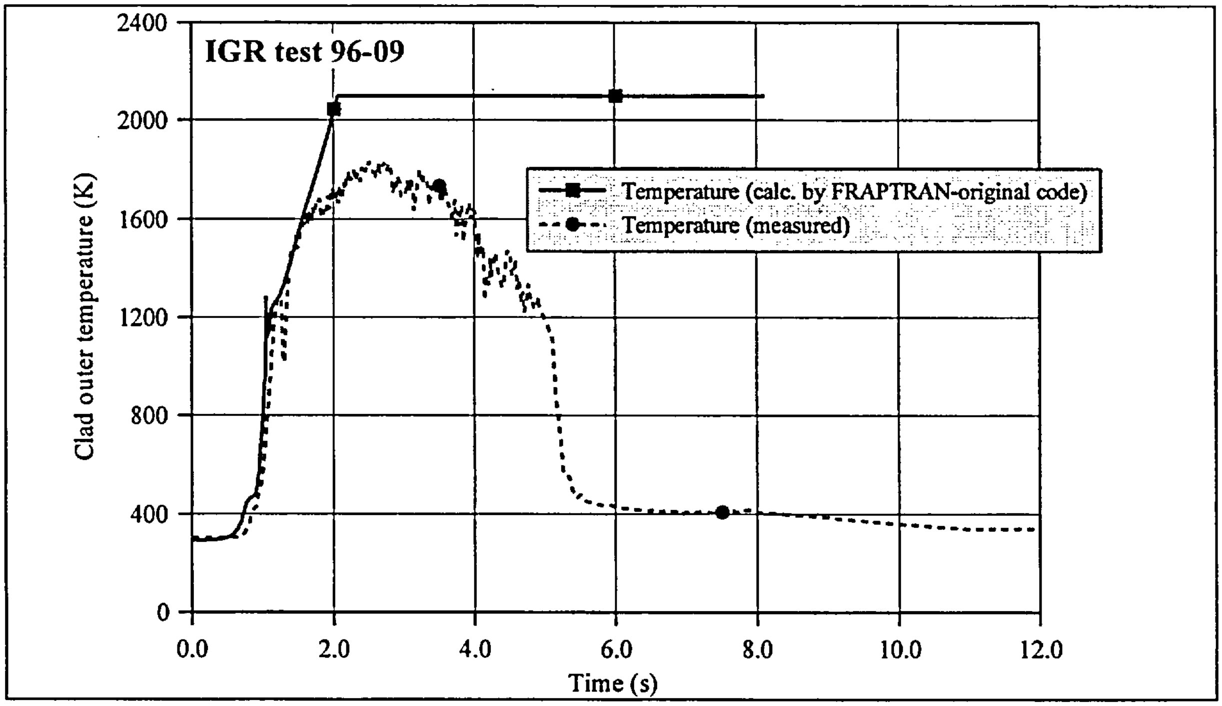

Fig. 7. Clad outer temperature in 96F-09 test calculated with Bromley-Pomerantz post-CHF heat transfer.

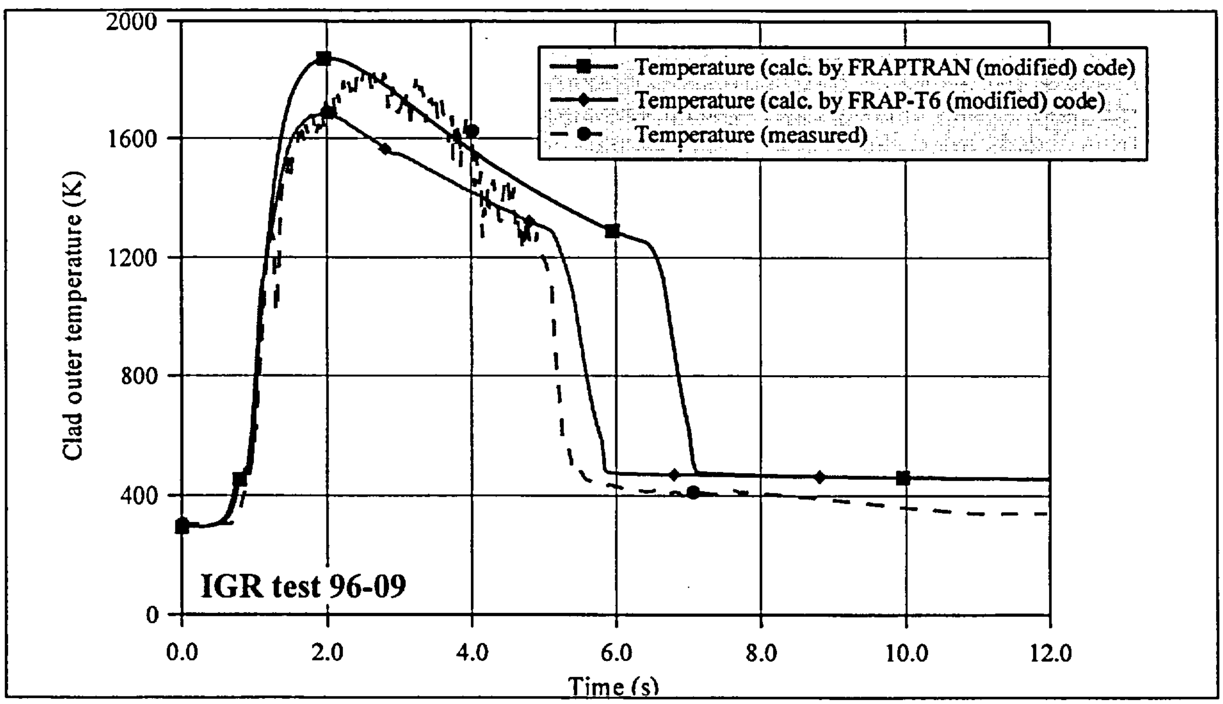

Fig. 8. Clad outer temperature in 96F-09 test calculated with Labuntzov post-CHF heat transfer.

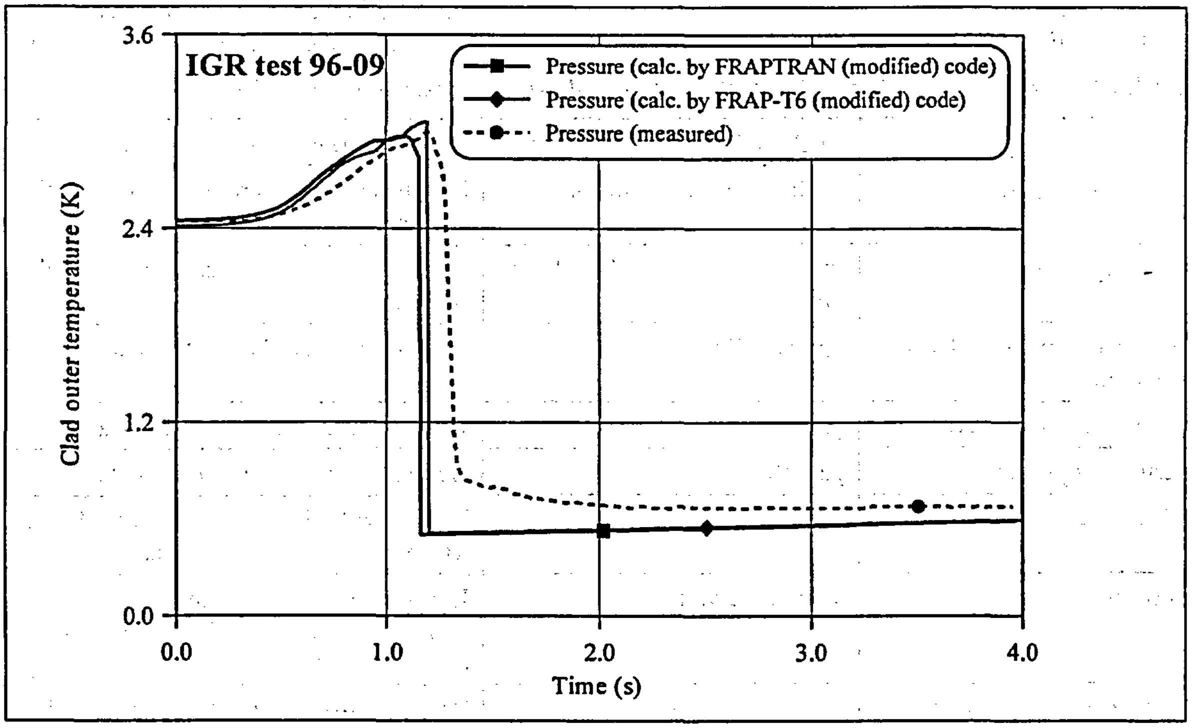

Fig. 9. Comparison of internal rod pressure in 96F-09 test, calculated with FRAP-T6 (modified) and FRAPTRAN (modified) codes.

4.1.4. High-burnup fuel simulation of IGR/RIA test

Earlier (see [30]), test fuel rod H5T was selected as an assessment case for the FRAPTRAN code. FRAPTRAN code developers conducted analysis of thermal mechanical parameters of fuel rod H5T, influence of fission gas release on thermal and mechanical behavior of the fuel rod. For boundary conditions for fuel rod calculation, rod-to-coolant heat-transfer coefficient at constant coolant temperature was assigned. In addition to that, initial data contained simplified fission gas release history, which did not account for transient gas swelling effect.

In this work, more detailed and refined method for assigning initial data for calculating high-burnup fuel using FRAPTRAN(modified) code is presented.

To predict behavior of high-burnup fuel rods, two methods for generating initial data are provided:

1. Calculation procedure providing for use of steady-state FRAPCON-3 code [28] for base irradiation regime. FRAPCON-3 code generates a calculation data array at the end of the base radiation, which serve as initial data for FRAPTRAN code.
2. Fuel rod calculation using FRAPTRAN code without FRAPCON-3 code. In this case, parameters of the fuel rod after the base operation in the reactor are assigned as initial data. Fuel and cladding parameters shall be obtained on the basis of post-irradiation examination of the fuel rod.

When analyzing calculation results, one should keep in mind that FRAPTRAN code does not calculate fission gas release (FGR) and transient swelling of the fuel matrix. To account for effects of fission gas release and transient swelling of fuel, initial data should include timetables for fission gas release and for the swelling of fuel pellets. In other words, temperature regime of the fuel rod does not affect fission gas release and swelling of the fuel. Dependencies of fission gas release and swelling vs. time were assigned on the basis of previous FRAP-T6 (modified) assisted calculations [3].

RIAR has conducted post-radiation studies of fuel rods irradiated in VVER-1000 reactor (5 unit of NVNPP) to the burnup of ~50 MWday/kg U. As a result, data on deformation of fuel and cladding, nuclide composition of fuel, cladding corrosion, fission gas release, etc. were obtained [3]. Therefore, to model behavior of burn-up fuel rods under IGR reactor conditions, calculation method not using FRAPCON-3 code was selected. For this case, method of initial data generation for FRAPTRAN code is presented in Table 15.

Table 15. Major input data for high-burnup fuel simulation needed for FRAPTRAN code.

Parameter	FRAPTRAN Input Variable	Source of the data
Cladding design data	RodDiameter, roughc, gapthk	Post base-irradiation test data of mother fuel rod
Fuel design data	FuelPelDiam, roughf, frden, rvoid	Post base-irradiation test data of mother fuel rod
Volume of upper and lower gas plenum	vplen, volbp	Before pulse-irradiation test data
Fraction of gas mixture	gfrac	Before pulse-irradiation test data
Internal gas pressure	gappr0	Before pulse-irradiation test data
FGR in transient	relfrac	User-specified FGR history from FRAP-T6 (modified) calculation data
Transient fuel swelling	TranFuelSwell	User-specified transient fuel swelling history from FRAP-T6 (modified) calculation data
Radially average fuel burnup	bup	Post base-irradiation test data of high-burnup fuel
Radial burnup profile	butemp	User-specified radial burnup profile from TRIFOB [31] calculation data
Normalized radial power profile	RadPowProfile	User-specified normalized radial power profile from TRIFOB calculation data
Oxide layer thickness	odoxid	Post base-irradiation test data of mother fuel rod
Excess hydrogen concentration	cexh2a	Post base-irradiation test data of mother fuel rod
Open porosity in fuel	OpenPorosityFraction	Determined by FRAPTRAN code

Similar approach was taken for assigning initial data for high-burnup fuel rods H7T and H1T tested in IGR reactor.

4.1.5. Calculated results of high-burnup fuel simulation obtained with modified FRAP-T6, SCANAIR and FRAPTRAN codes

The calculation results for high-burnup fuel rods H5T, H7T, H1T are presented below in Fig. 10–Fig. 21. The FRAPTRAN (modified) results are compared with results computed by the SCANAIR (modified) and FRAP-T6 (modified) codes. Considering that the applied SCANAIR version [32] had no model of cladding deformation of the ballooning type and respective failure models, calculation results obtained by SCANAIR code are presented to the point of initiation of clad plastic deformation after the re-opening of gas gap.

High-burnup fuel simulation of IGR/RIA test (H5T assessment case)

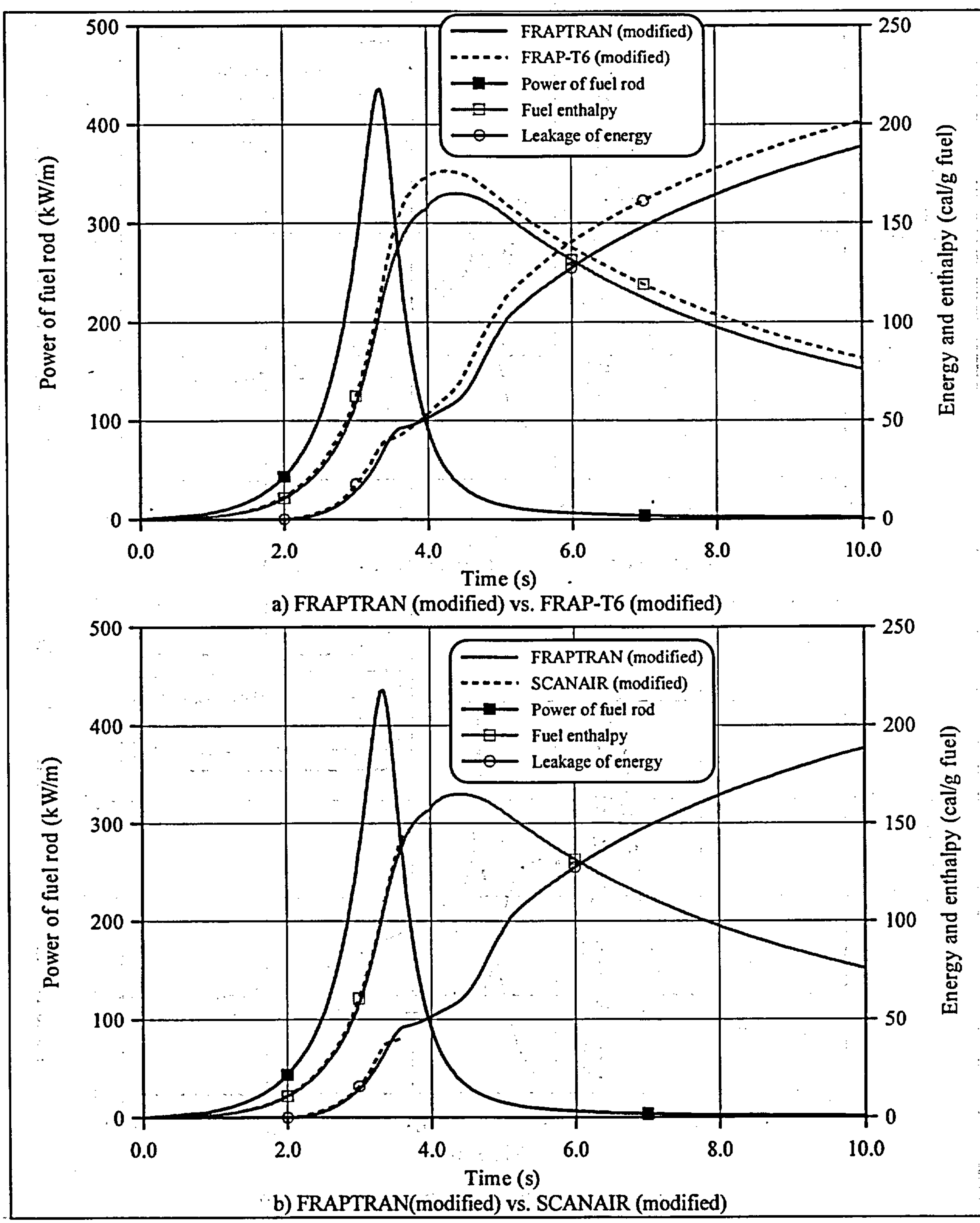

Fig. 10. Energy characteristics vs. time calculated by modified FRAP-T6, SCANAIR and FRAPTRAN codes (H5T test case).

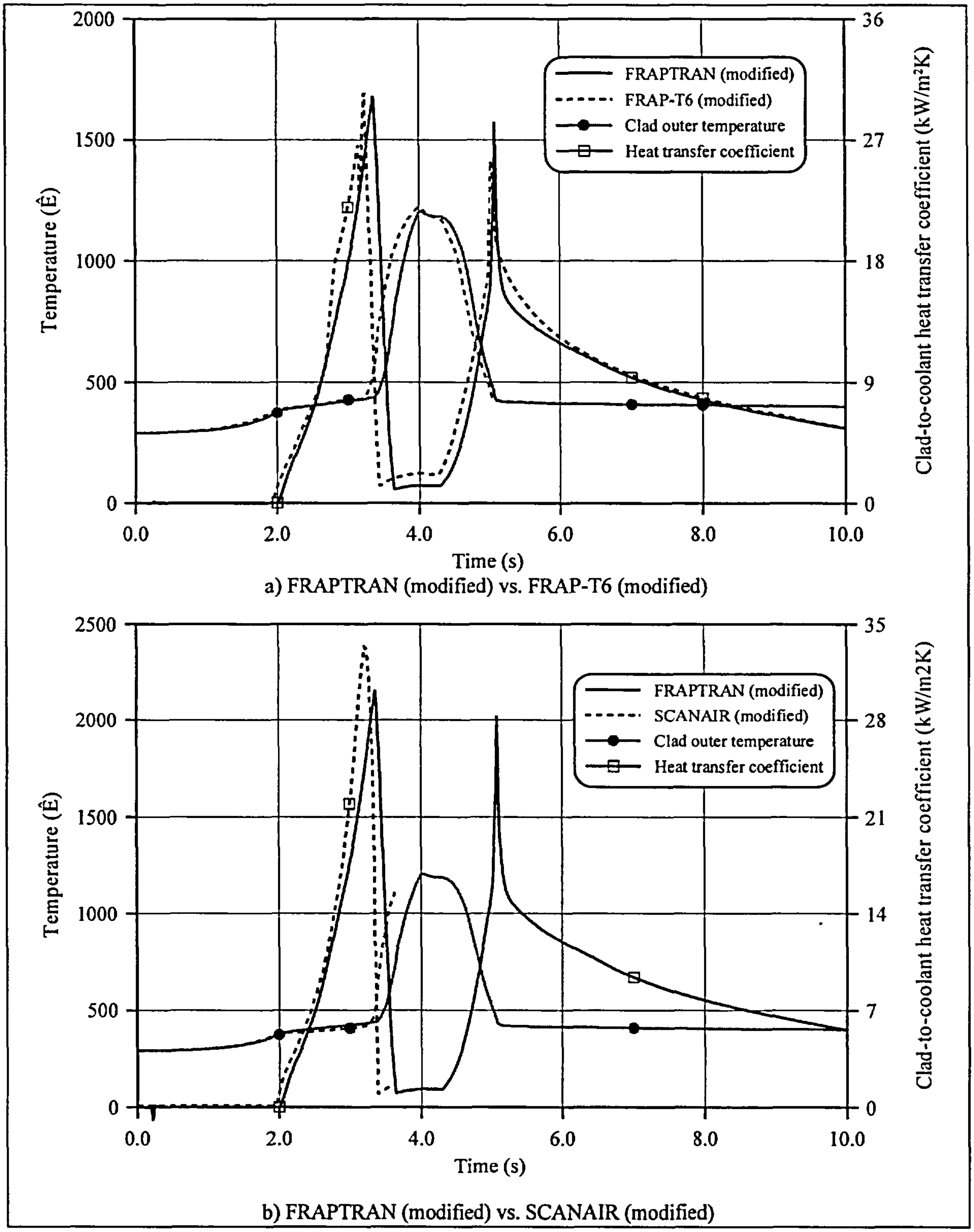

Fig. 11. Cladding temperatures and heat transfer coefficients vs. time calculated by modified FRAP-T6, SCANAIR and FRAPTRAN codes (H5T test case).

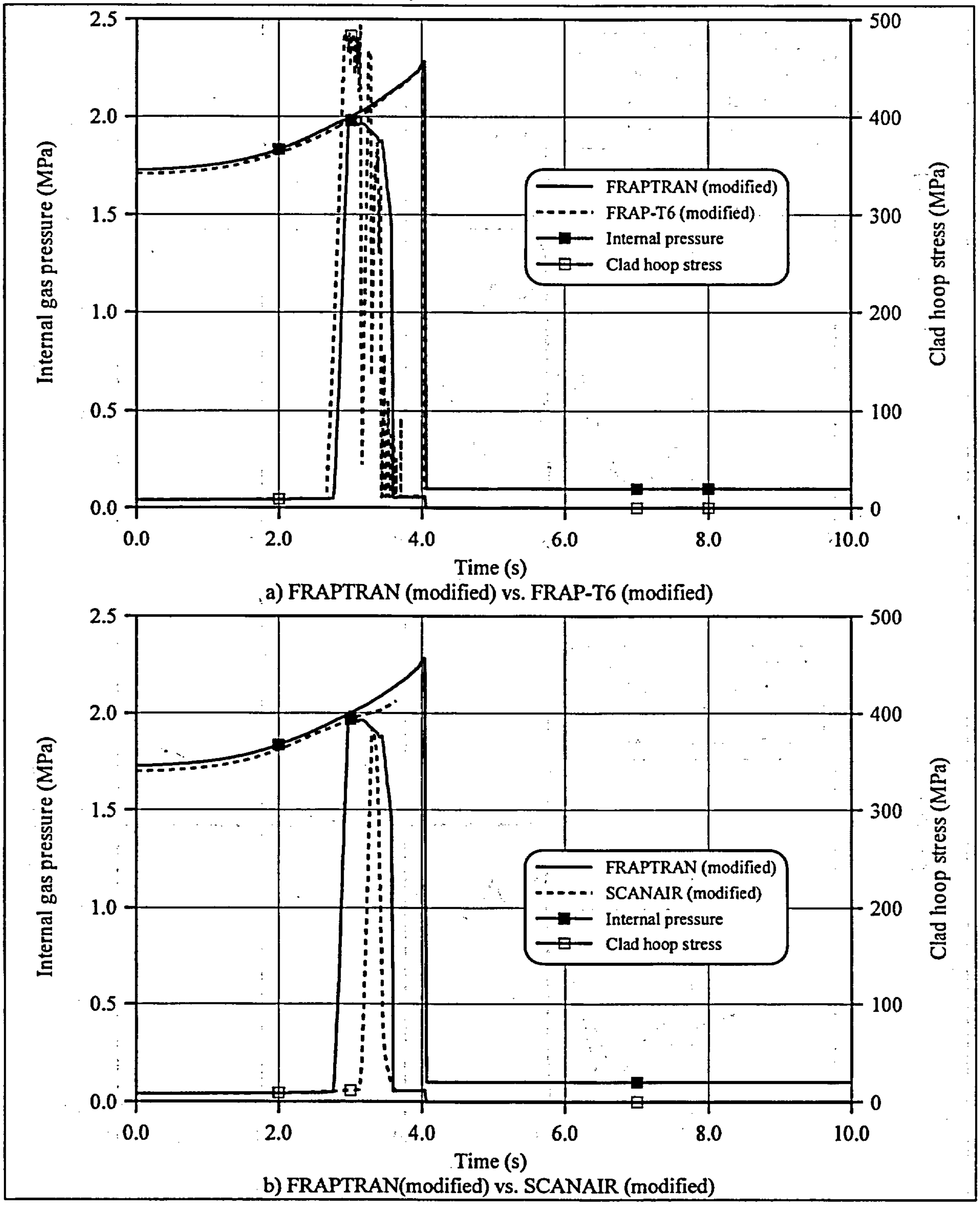

Fig. 12. Cladding hoop stresses and internal pressures vs. time calculated by modified FRAP-T6, SCANAIR and FRAPTRAN codes (H5T test case).

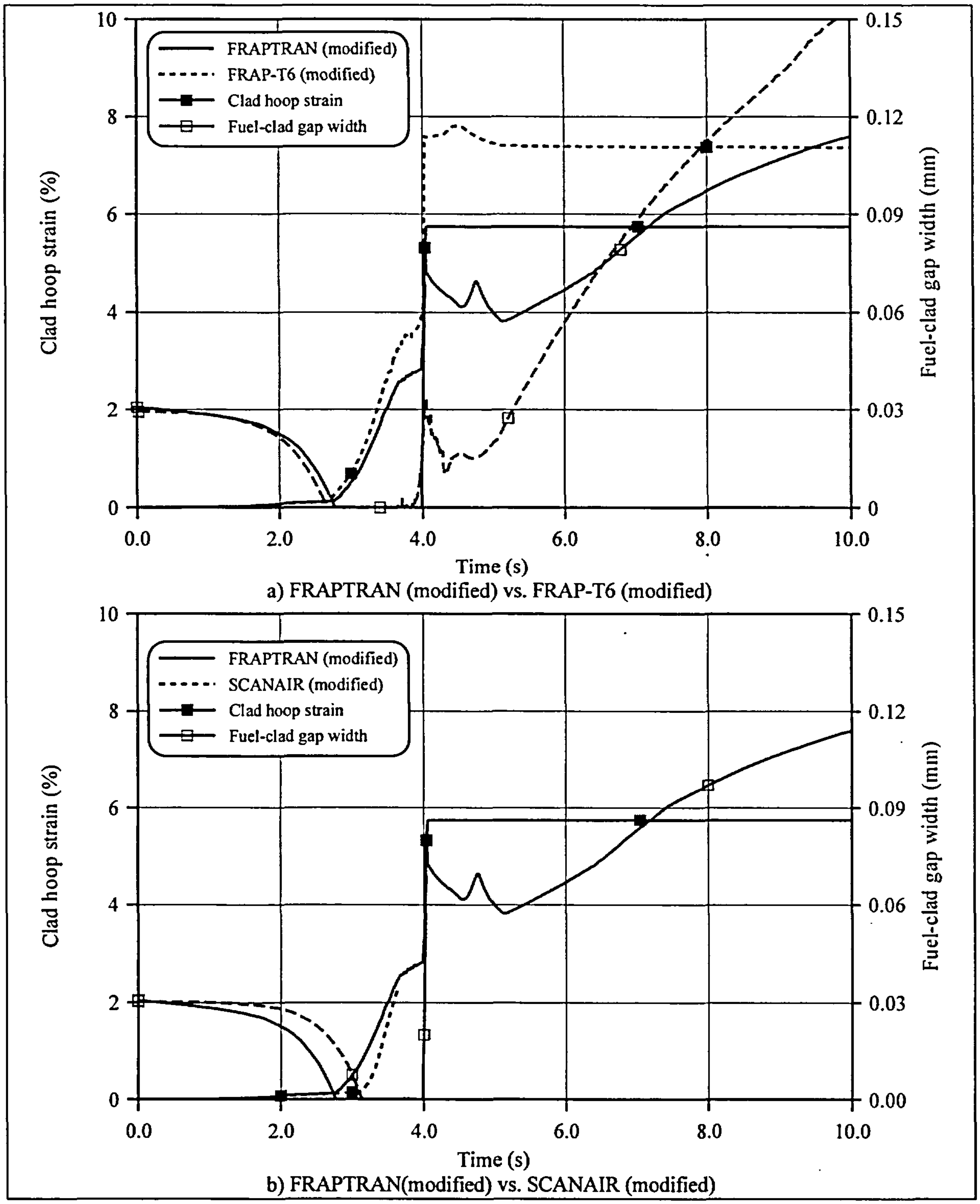

Fig. 13. Cladding hoop strains and gap widths vs. time calculated by modified FRAP-T6, SCANAIR and FRAPTRAN codes (H5T test case).

High-burnup fuel simulation of IGR/RIA test (H7T assessment case)

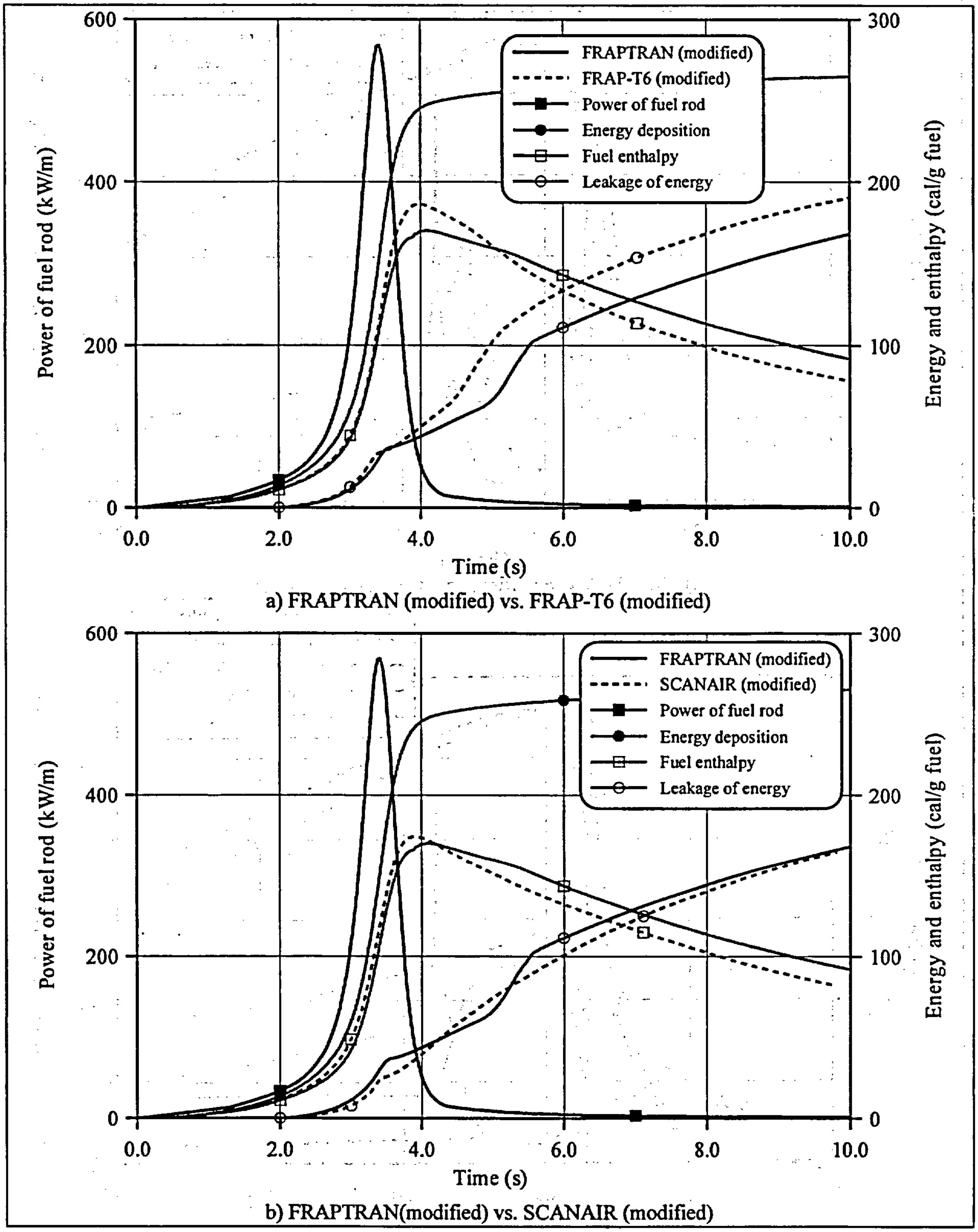

a) FRAPTRAN (modified) vs. FRAP-T6 (modified)

b) FRAPTRAN(modified) vs. SCANAIR (modified)

Fig. 14. Energy characteristics vs. time calculated by modified FRAP-T6, SCANAIR and FRAPTRAN codes (H7T test case).

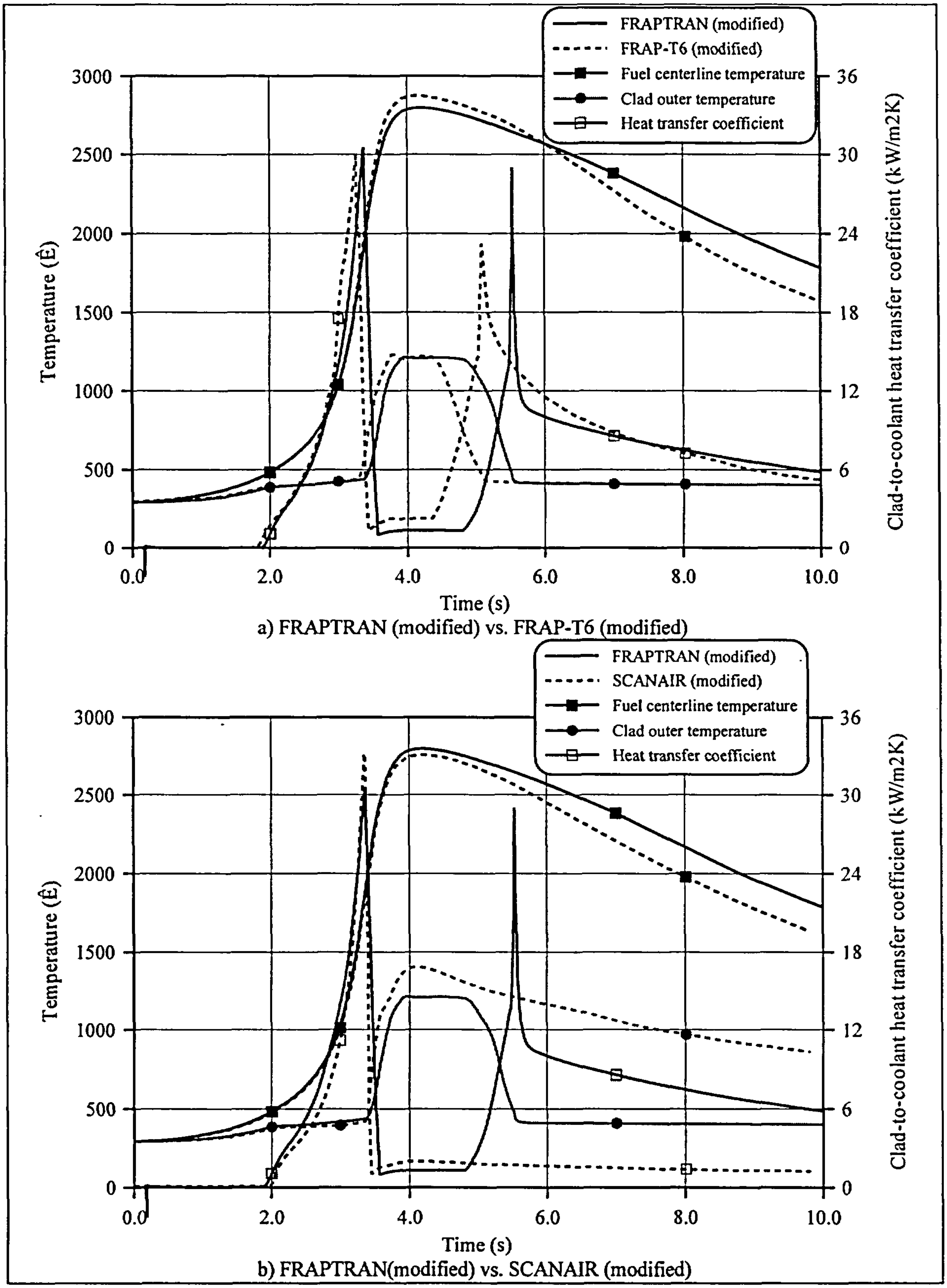

Fig. 15. Cladding temperatures and heat transfer coefficients vs. time calculated by modified FRAP-T6, SCANAIR and FRAPTRAN codes (H7T test case).

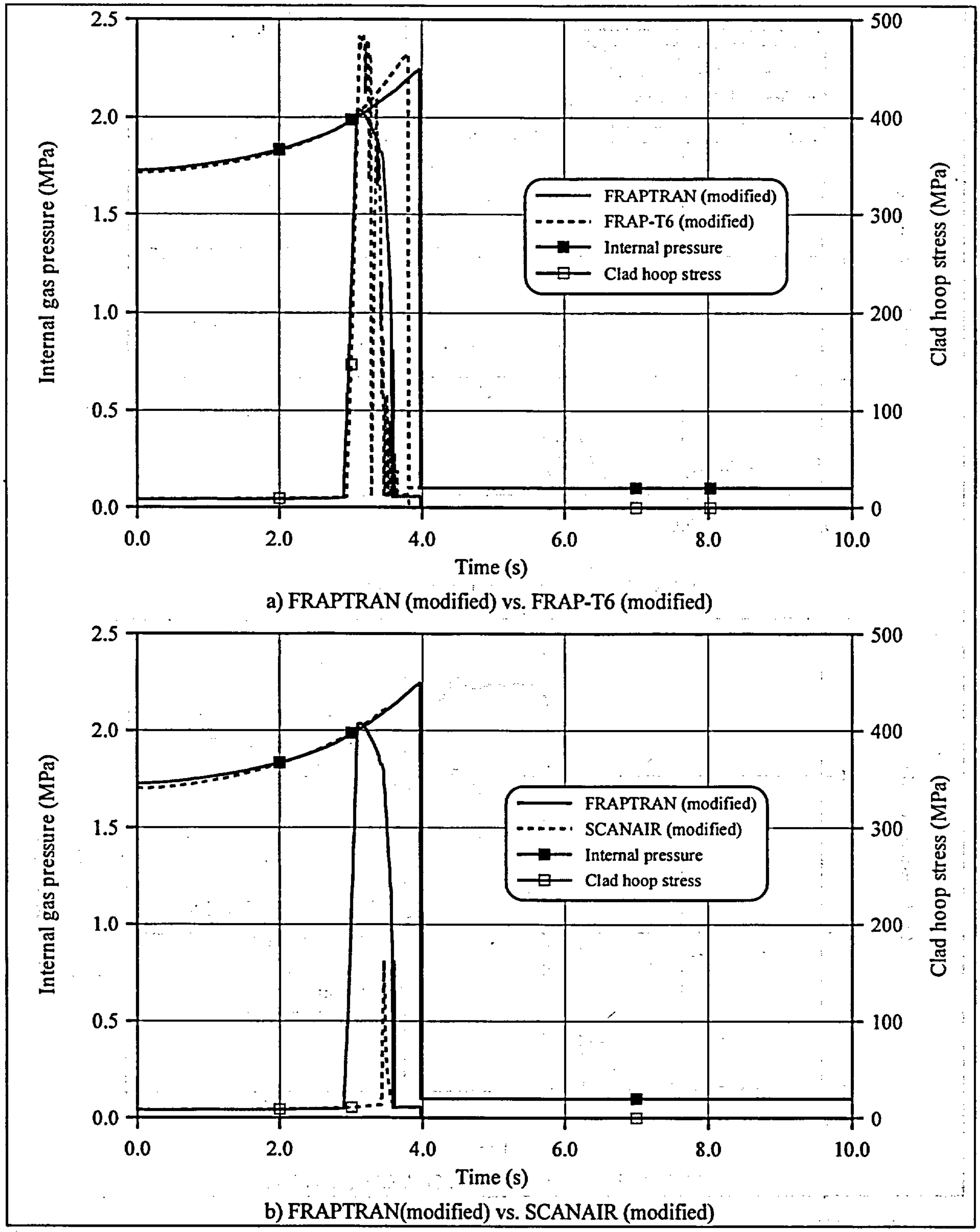

Fig. 16. Cladding hoop stresses and internal pressures vs. time calculated by modified FRAP-T6, SCANAIR and FRAPTRAN codes (H7T test case).

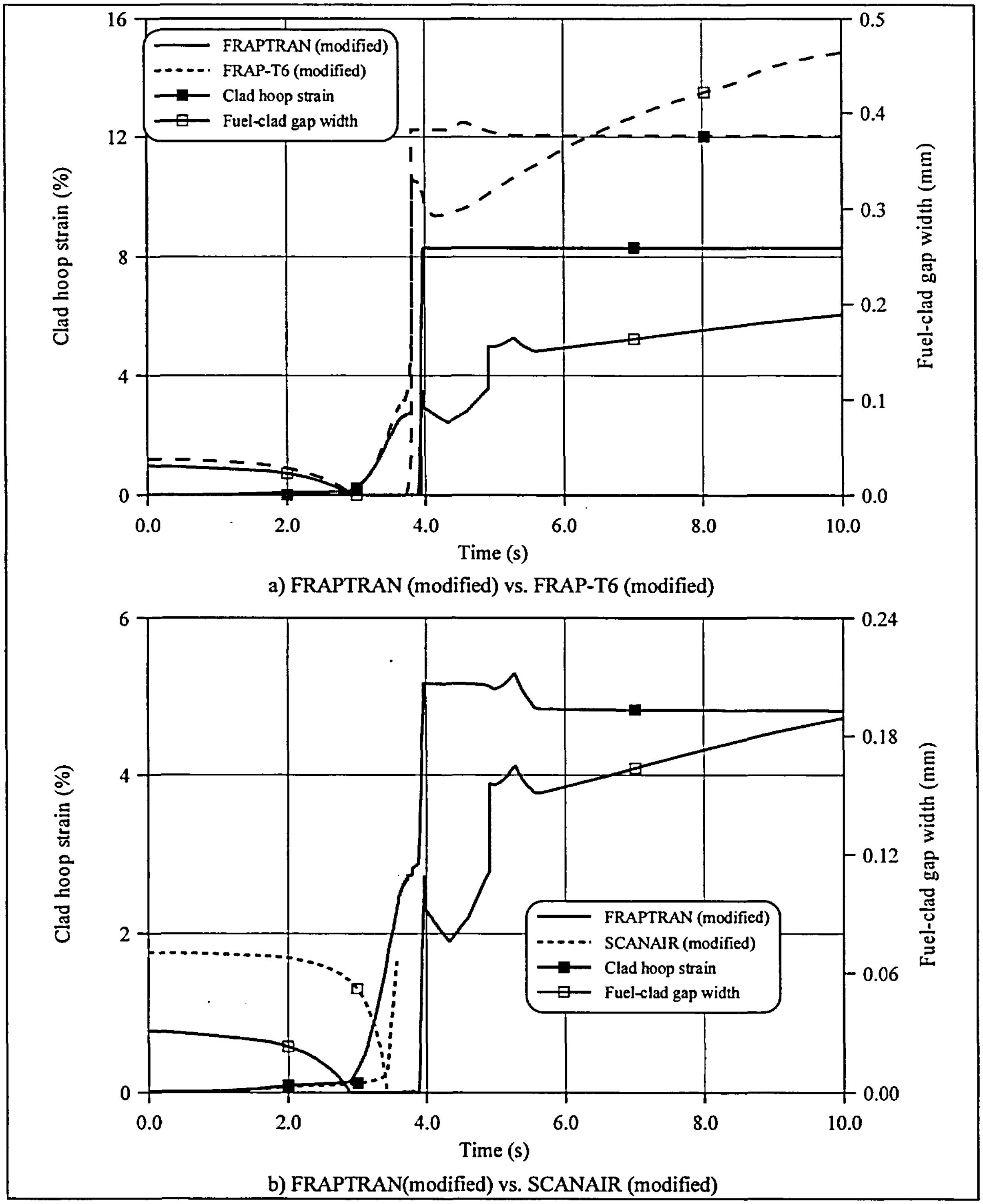

Fig. 17. Cladding hoop strains and gap widths vs. time calculated by modified FRAP-T6, SCANAIR and FRAPTRAN codes (H7T test case).

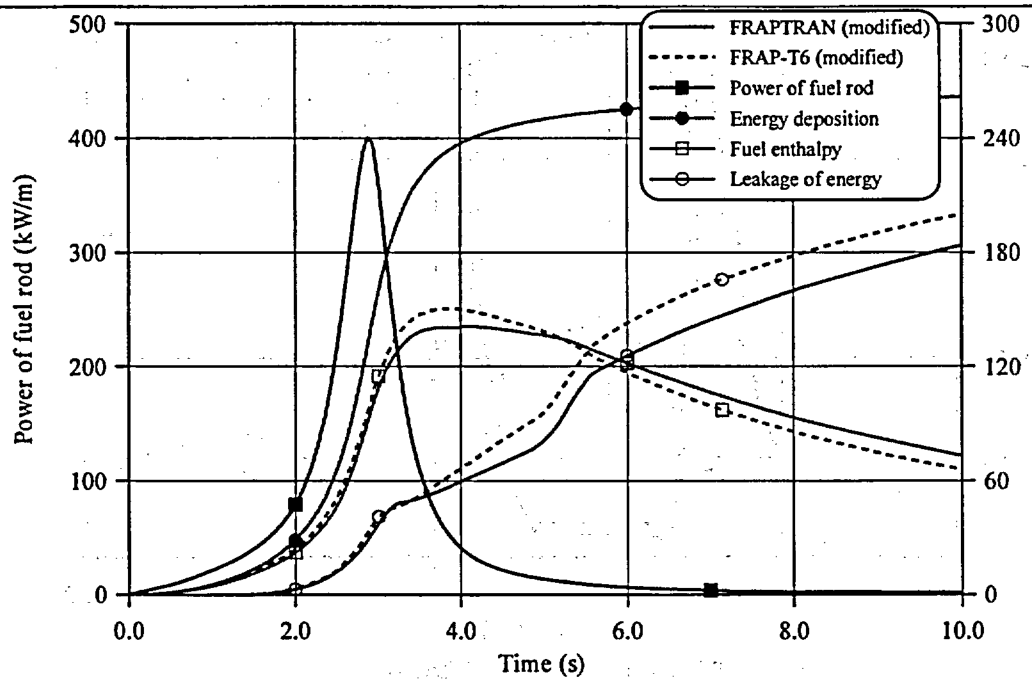

a) FRAPTRAN (modified) vs. FRAP-T6 (modified)

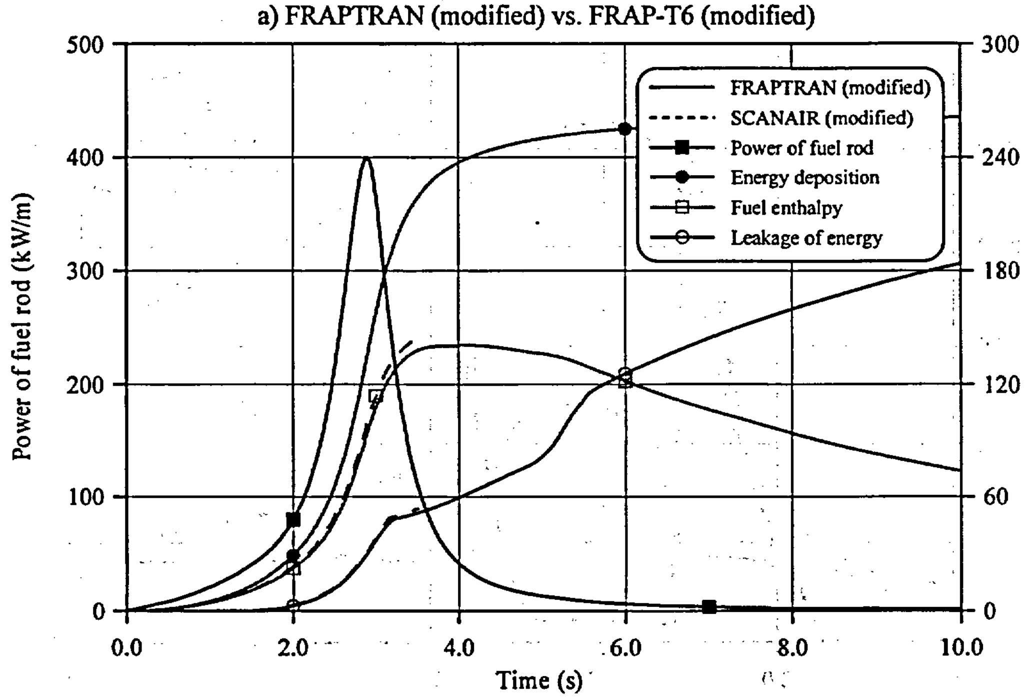

b) FRAPTRAN(modified) vs. SCANAIR (modified)

Fig. 18. Energy characteristics vs. time calculated by modified FRAP-T6, SCANAIR and FRAPTRAN codes (H1T test case).

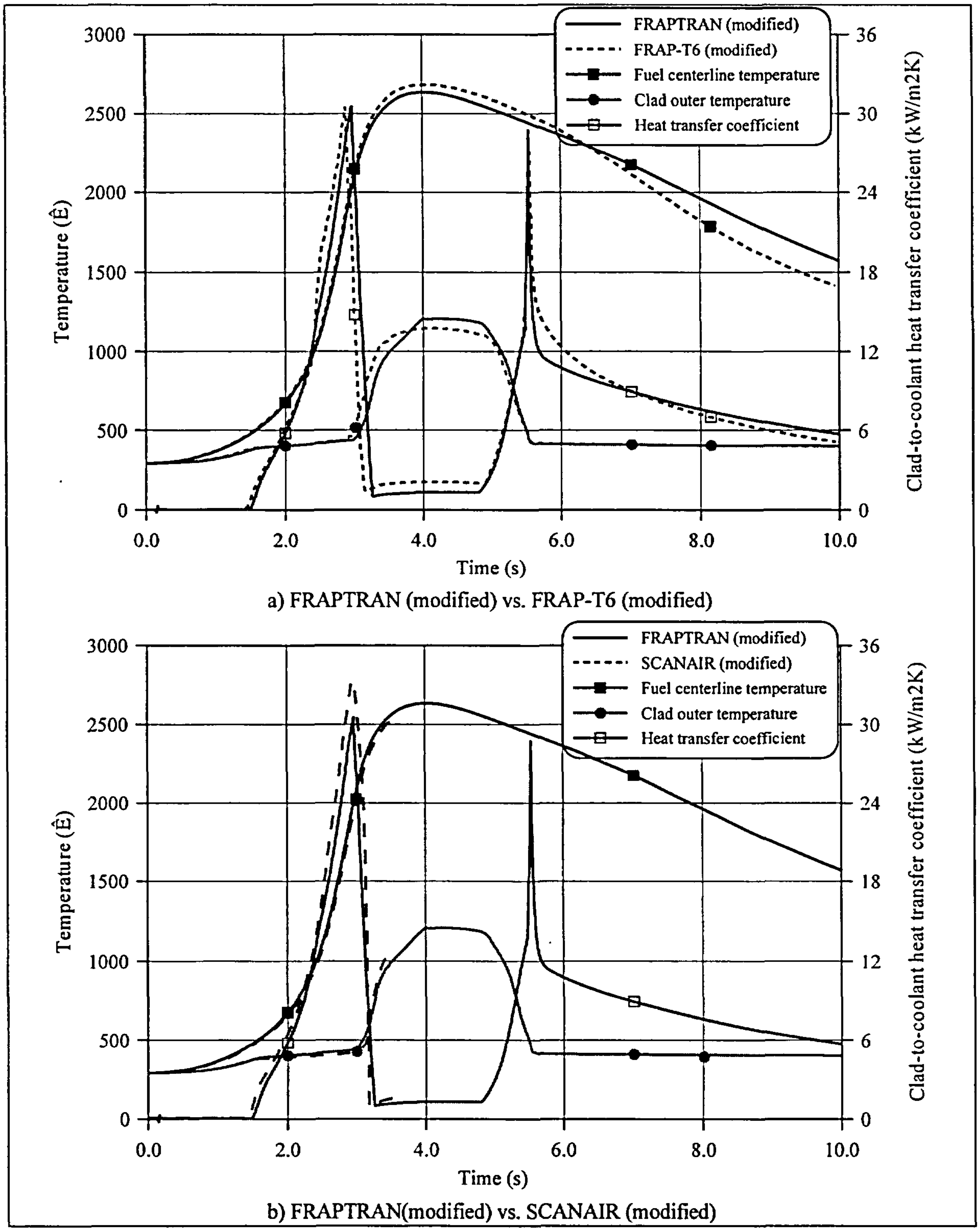

Fig. 19. Cladding temperatures and heat transfer coefficients vs. time calculated by modified FRAP-T6, SCANAIR and FRAPTRAN codes (H1T test case).

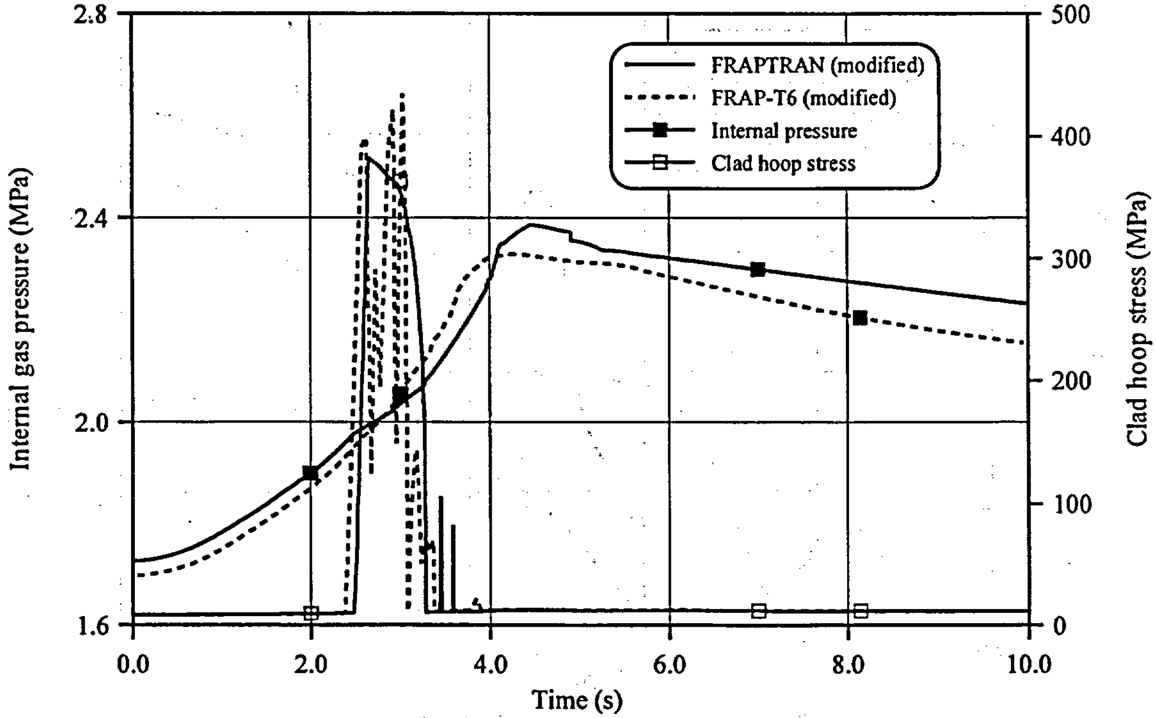

a) FRAPTRAN (modified) vs. FRAP-T6 (modified)

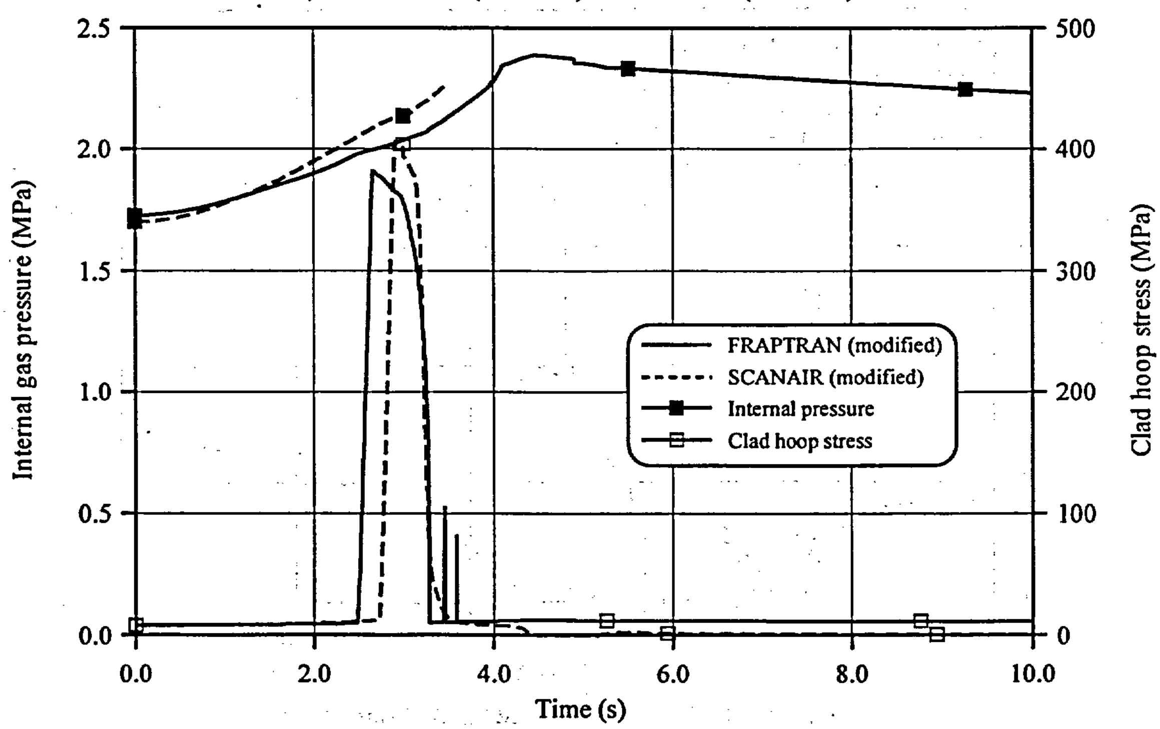

b) FRAPTRAN(modified) vs. SCANAIR (modified)

Fig. 20. Cladding hoop stresses and internal pressures vs. time calculated by modified FRAP-T6, SCANAIR and FRAPTRAN codes (H1T test case).

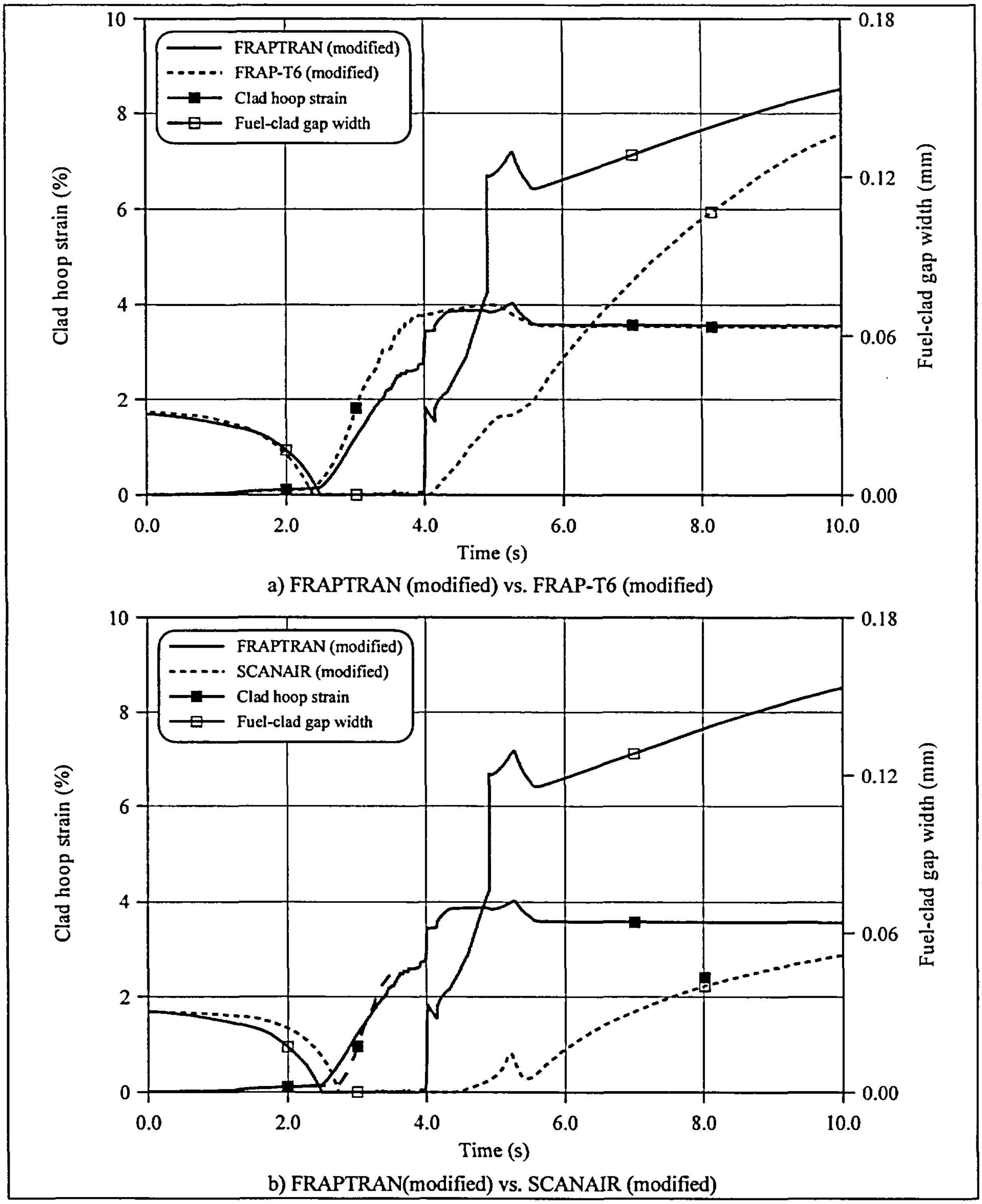

a) FRAPTRAN (modified) vs. FRAP-T6 (modified)

b) FRAPTRAN(modified) vs. SCANAIR (modified)

Fig. 21. Cladding hoop strains and gap widths vs. time calculated by modified FRAP-T6, SCANAIR and FRAPTRAN codes (H1T test case).

4.1.6. Discussion of principal thermal parameters calculated by the codes

Comparison of the above results of IGR test calculations of FRAP-T6 and FRAPTRAN codes shows that peak fuel enthalpy calculated by FRAP-T6 code systematically exceeds the value of peak fuel enthalpy obtained by FRAPTRAN code. Performed analysis revealed that the main reason for such discrepancy is quantitative difference of fuel-cladding gap thermal conductivity models, which determine the fuel-to-cladding energy leakage.

Calculations of fuel-cladding gap thermal conductivity can be performed by both FRAP-T6 and FRAPTRAN codes using Ross-Stoute model. The difference between the models is in the use of different empiric coefficients (Table 16).

General form of thermal conductivity of fuel-cladding system is given by:

$$\alpha_{gap} = \alpha_{gas} + \alpha_{solid} + \alpha_{rad},$$

where α_{gas} – thermal conductivity through the gas gap between fuel and cladding (W/m^2 K);

α_{solid} – thermal conductivity due to fuel-cladding contact pressure (W/m^2 K);

α_{rad} – thermal conductivity due to radiation (W/m^2 K).

Table 16. Comparison of fuel-cladding gap thermal conductivity models in FRAP-T6 and FRAPTRAN codes.

	Model content	
	FRAP-T6(modified)	*FRAPTRAN*
α_{gas}	$\dfrac{\lambda_g}{\Delta + (R_f + R_c) + (g_f + g_c)}$	$\dfrac{\lambda_g}{\Delta + 3.6(R_f + R_c) + (g_f + g_c)}$
	λ_g - gas thermal conductivity (W/m-K); Δ - hot fuel-cladding gas gap (m); R_f - fuel surface roughness (m); R_c - cladding surface roughness (m); g_f+g_c - combined fuel and cladding temperature jump distance (m)	
α_{solid}	$4.5579\cdot10^{-3}\dfrac{k_m P_{rel}^n}{R\cdot E}A$ A = coefficient dependent upon P_{rel} A=0.01, if $0.01 \ge P_{rel} \ge 0.0001$ A=1, if $P_{rel} < 0.0001$ or $P_{rel} > 0.01$ P_{rel} = ratio of interfacial pressure to cladding Meyer hardness n = exponent dependent upon P_{rel} n=0, if $0.01 \ge P_{rel} \ge 0.0001$ n=0.5, if $P_{rel} < 0.0001$ n=1, if $P_{rel} > 0.01$ K_m = mean thermal conductivity of fuel and cladding (W/m-K) $K_m = 2K_f K_c/(K_f+K_c)$ where K_f and K_c are the fuel and cladding thermal conductivities, respectively, evaluated at their respective surface temperatures $R = (R_f^2 + R_c^2)^{0.5}$ where R_f and R_c are the fuel and cladding surface roughness, respectively (m) $E = \exp[5.738 - 0.528\cdot\ln(3.937\cdot10^7)]$	$0.4166\,K_m P_{rel}^{0.5}/(R\cdot E)$, if $P_{rel} < 9\cdot10^{-6}$ $0.00125\cdot K_m/(R\cdot E)$, if $0.003 > P_{rel} > 9\cdot10^{-6}$ $0.4166\dfrac{K_m P_{rel} R_{mult}}{R\cdot E}$, if $P_{rel} > 0.003$ $R_{mult} = 333.3\cdot P_{rel}$, if $P_{rel} < 0.0087$ $R_{mult} = 2.9$, if $P_{rel} > 0.0087$ P_{rel} = ratio of interfacial pressure to cladding Meyer hardness K_m = mean thermal conductivity of fuel and cladding (W/m-K) $K_m = 2K_f K_c/(K_f+K_c)$ where K_f and K_c are the fuel and cladding thermal conductivities, respectively, evaluated at their respective surface temperatures $R = (R_f^2 + R_c^2)^{0.5}$ where R_f and R_c are the fuel and cladding surface roughness, respectively (m) $E = \exp[5.738 - 0.528\cdot\ln(R_f a)]$ where $a = 3.937\cdot10^7$ μm
α_{rad}	$(T_f^2+T_c^2)\cdot(T_f+T_c)\cdot F_e\cdot F_a\cdot\sigma$ σ = Stefan-Boltzmann constant = $5.6697\cdot10^{-8}$ W/m^2-K^4 F_e = emissivity factor determined by MATPRO F_a = configuration factor = 1.0 T_f = temperature of fuel outer surface (K) T_c = temperature of cladding inner surface (K)	

To verify the influence of conductivity models on thermal parameters of fuel rods, gap conductivity model from FRAP-T6/VVER was incorporated into the FRAPTRAN code. Then comparative analysis of fuel temperature, cladding temperature and peak fuel enthalpy was performed by the example of fuel rod H5T. The effect of gap thermal conductivity is illustrated in Fig. 22. Note that conductivity of the gap (contact) calculated using FRAPTRAN (original) model exceed values of conductivity obtained using FRAP-T6 model up to the 4[th] second of the process. Then, re-opening of the gap occurs, and influence of conductivity effect from this point on is insignificant.

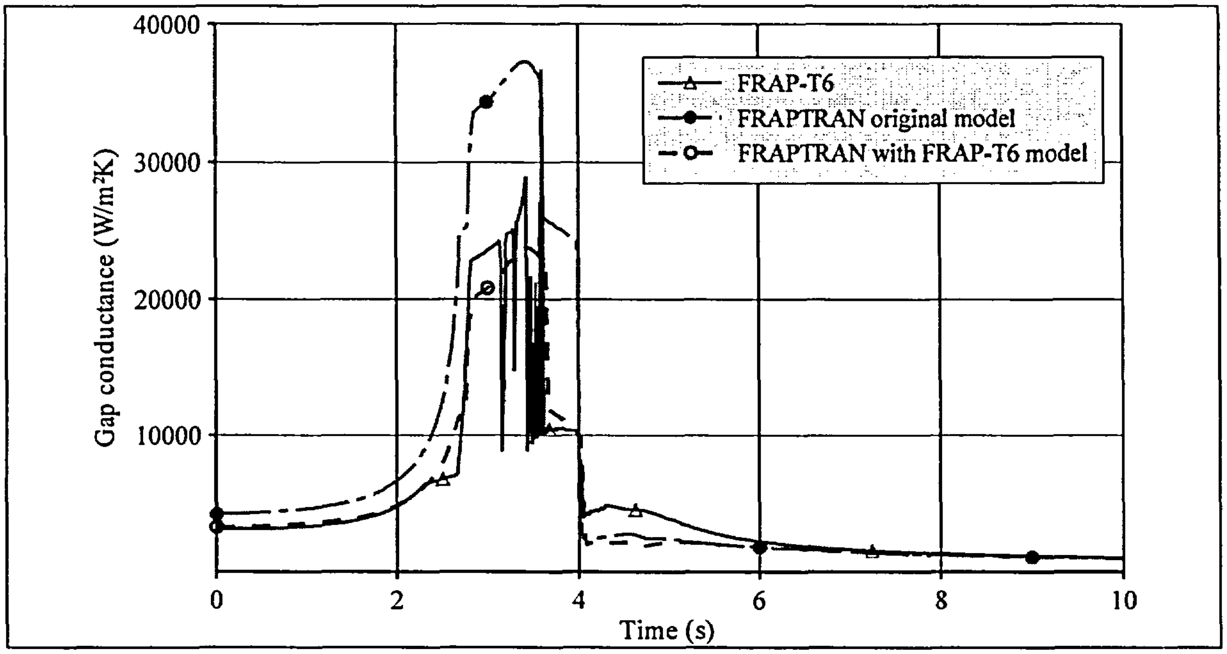

Fig. 22. Comparison of gap thermal conductivity models from FRAP-T6 (modified) and FRAPTRAN (modified) and FRAPTRAN (original).

Thus, gas component of fuel-cladding gap thermal conductivity used in FRAPTRAN code gives higher values as compared with FRAP-T6 code. This results in increase of fuel-to-cladding heat flow (energy leakage). Due to this, fuel temperature (peak fuel enthalpy) goes slightly down as compared with calculated temperature obtained using FRAP-T6 code. Level of peak fuel enthalpy decrease due to the usage of two conductivity models is shown in Fig. 23.

Fig. 24 displays comparison of calculated results obtained using FRAP-T6 and FRAPTRAN codes, which has the same conductivity model from FRAP-T6. It was shown that in this case, heat flow and energy leakage from the fuel rod go down, and therefore, peak fuel enthalpy goes up.

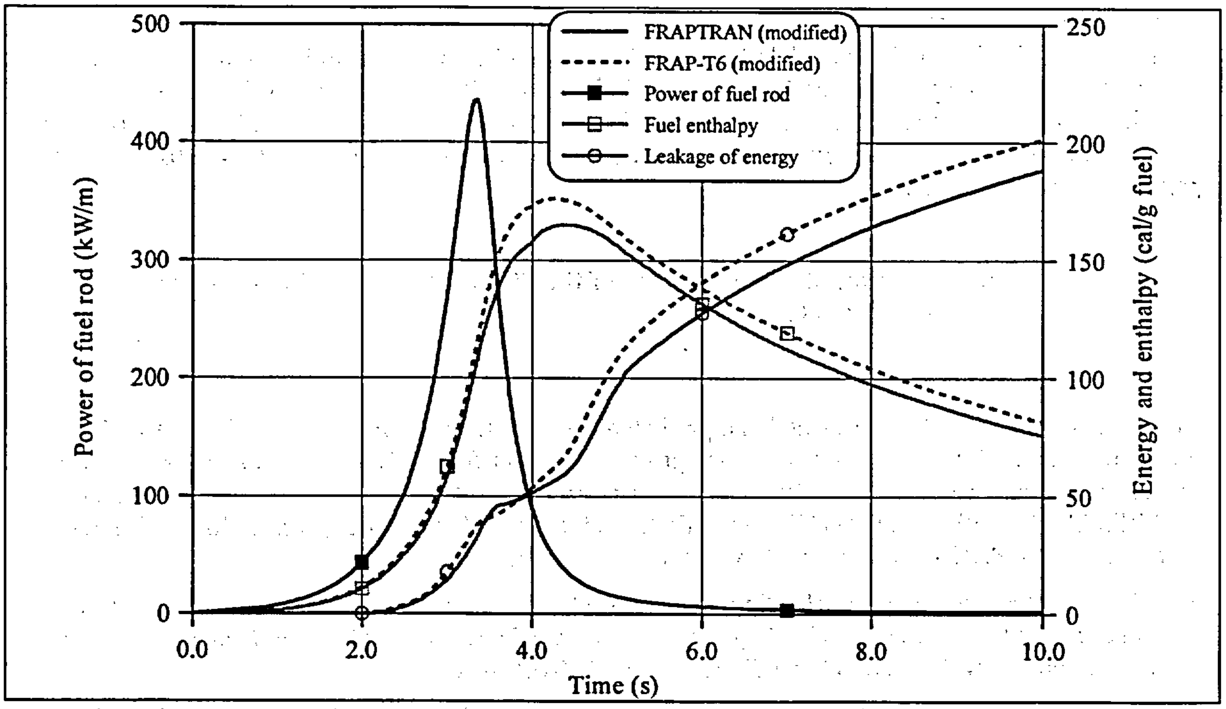

Fig. 23. Peak enthalpy calculated by FRAP-T6 (modified) and FRAPTRAN (modified).

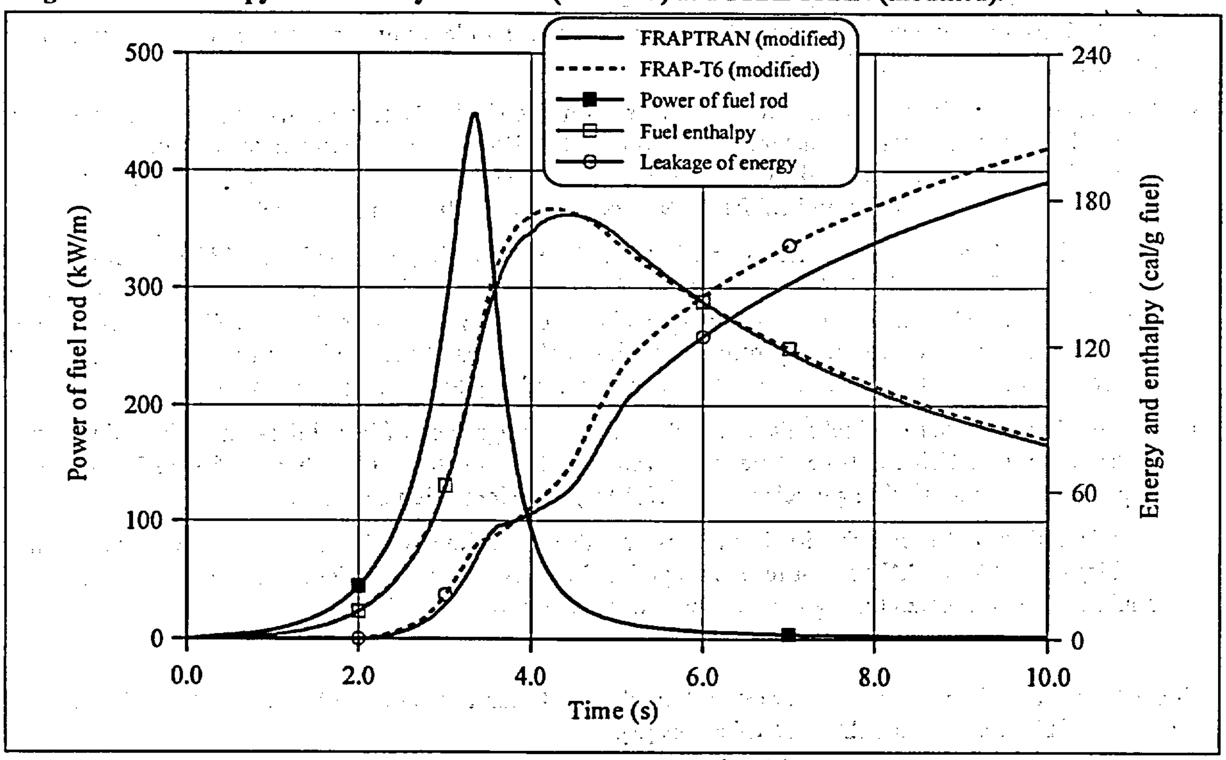

Fig. 24. Peak enthalpy calculated by FRAP-T6 (modified) and FRAPTRAN (modified) with gap thermal conductivity model from FRAP-T6 (modified).

Moreover, by the example of calculation results for test rods with fresh fuel 50F16 (see Fig. 6) and 96F09 (see Fig. 8), it was shown that influence of fuel-cladding gap thermal conductivity on cladding temperature is significantly higher. Increase of maximum cladding temperature in the case of modeling using modified FRAPTRAN code is 80 K for fuel rod 50F16 and 120K for fuel rod 96F09 as compared with results obtained by the modified FRAP-T6 code.

In the future, selection of either model of gap conductivity under conditions of high-temperature contact of fuel and cladding (especially for high-burnup fuel rods) will have to be confirmed by appropriate experimental data. In other words, empirical coefficients have to be selected on the basis of experimental data, which correspond to the given type and state of the fuel rod, as well as taking into consideration particular conditions of its operation.

4.1.7. Summary of the assessment of the FRAPTRAN (modified) against RIA-simulated test data

Comparative analyses of experimental and predicted cladding temperatures were carried out in the energy deposition range of 120-400 cal/g. Assessment cases of fresh fuel rods were compared with in-pile test measurements and calculated results of cladding temperature at rod outer surface. The comparison of FRAPTRAN (modified), SCANAIR (modified) and FRAP-T6 (modified) predictions with test data obtained from IGR/RIA experiments show that (see Table 17):

- The predicted and measured cladding temperature histories are in satisfactory agreement. However, it is necessary to mention that cladding temperatures predicted with FRAPTRAN (modified) are higher than computed with FRAP-T6 (modified) and SCANAIR (modified).
- Comparison of fuel and cladding behavioral models was performed in FRAP-T6 and FRAPTRAN. As a result it was shown that decrease in peak fuel enthalpy in the assessment cases under consideration resulted from differences in empirical coefficients in fuel – cladding gap thermal conductivity models of the FRAP-T6 and FRAPTRAN.
- Simulation of high-burnup fuel rod behavior with FRAPTRAN (modified) showed that the main thermal and mechanical parameters of fuel rods H1T, H5T, H7T are similar to previous calculation with FRAP-T6 (modified) and SCANAIR (modified). However the overprediction of the cladding temperature was obtained with FRAPTRAN (modified), as well as for fresh fuel rods.
- FRAPTRAN (modified) has correctly predicted failure of cladding of rods H5T, H7T and preservation of integrity of test rod H1T. No systematic differences of FRAPTRAN predictions of maximum hoop strain of the cladding from the calculated data obtained earlier have been detected. Certain discrepancy of data on deformation can result from correlation differences of mechanical properties in the updated version of MATPRO, as well as from differences in cladding temperature history predictions.
- In modeling high-burnup fuel rods, the problems with assignment of initial data on radial-axial burnup distribution (BUTEMP), time dependent transient fuel swelling (TRANFUELSWELL) and time dependent transient fission gas release (RELFRAC) were identified and resolved.
- In calculating fuel rods behavior in the power pulse conditions, difficulties with solving mechanical problem in FRAPTRAN code at re-opening of fuel-cladding gap were identified. At that, the problems could not be eliminated through mere decrease of time step.

Table 17. Comparison of main thermal and mechanical results predicted by the modified FRAP-T6, SCANAIR and FRAPTRAN codes [3].

Parameter	Unit	Experiment	SCANAIR (modified)	FRAP-T6 (modified)	FRAPTRAN (modified)
H5T (49.0 MWd/kg U)					
Peak fuel enthalpy	Cal/g	-	-	176	172
Peak fuel temperature	K	-	-	2817	2834
Peak clad temperature	K	-	-	1224	1220

Parameter	Unit	Experiment	SCANAIR (modified)	FRAP-T6 (modified)	FRAPTRAN (modified)
Cladding failure		yes	-	yes	yes
Residual clad hoop strain (ballooning region)	%	6.5	-	7.28	5.75
H7T (47.3 MWd/kg U)					
Peak fuel enthalpy	Cal/g	-	-	187	172
Peak fuel temperature	K	-	-	2876	2797
Peak clad temperature	K	-	-	1231	1222
Cladding failure		yes	-	yes	yes
Residual clad hoop strain (ballooning region)	%	10.1	-	11.9	7.71
H1T (49.2 MWd/kg U)					
Peak fuel enthalpy	Cal/g	-	147	151	146
Peak fuel temperature	K	-	2601	2681	2676
Peak clad temperature	K	-	1192	1148	1207
Cladding failure		no	-	no	no
Residual clad hoop strain*	%	1.4	1.83	2.82	2.94
Maximum clad hoop strain**	%	-	2.24	3.43	3.58

4.2. RIAR/LOCA assessment

4.2.1. Description of experiments modeling the first stage of LOCA

Special facility with heating of a fuel rod by means of direct transmission of electric current through cladding (Fig. 25) has been developed at RIAR for testing simulators of unirradiated and irradiated fuel rods under conditions, which model initial stages of LOCA [29]. This facility permitted to conduct experiments necessary for verifying that behavior of cladding of real fuel rod with complicated geometry, which is subjected to a complex set of loading factors, would correlate with the results achieved in significantly less complicated biaxial burst tests.

* Axially averaged clad hoop strain

** Local clad hoop strain along fuel rod height

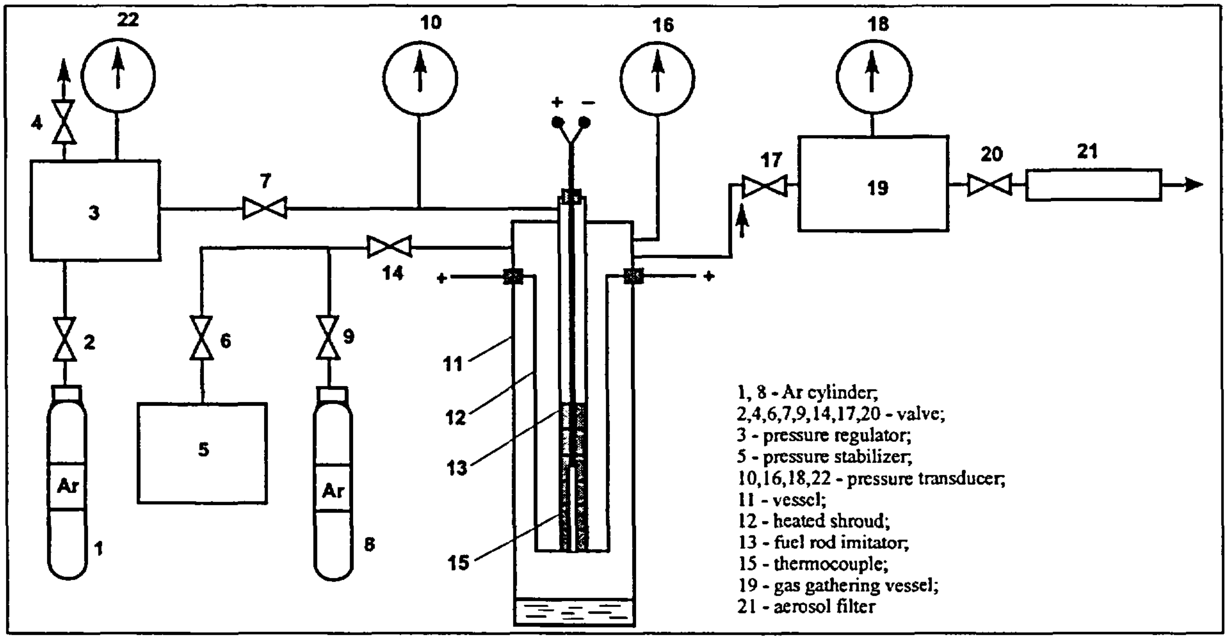

Fig. 25. Schematic diagram of electrically heated facility for studying the first stage of LOCA.

Scenarios of temperature change and pressure drop at the cladding of fuel rod simulator tested at RIAR (RIAR-LOCA2), are shown in Fig. 26 [29].

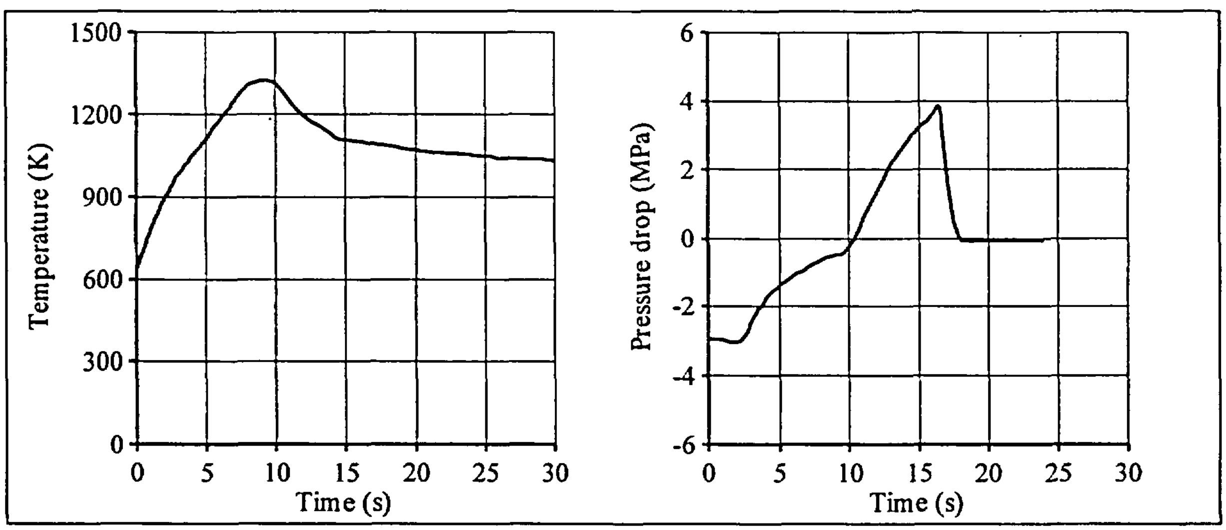

Fig. 26. Simulator cladding temperature and cladding pressure drop.

Fuel rod simulator consisted of cladding (Zr-1%Nb) and fuel stack. Geometry of Al_2O_3 fuel pellets was the same as for VVER-1000 fuel. Simulator was filled with argon under constant pressure, which was maintained at the set level with the help of pressure stabilizer. Required scenario of pressure drop change at the cladding was ensured by means of coolant (argon) pressure variation.

In the course of each test, the following parameters were measured:

- coolant pressure;
- pressure in the simulator;
- cladding temperature.

In addition, during the stage of post-test examinations hoop strain versus axial length and parameters of burst region of the cladding were measured. Appearance and cross-section of the simulator after the test are shown in Fig. 27 [29].

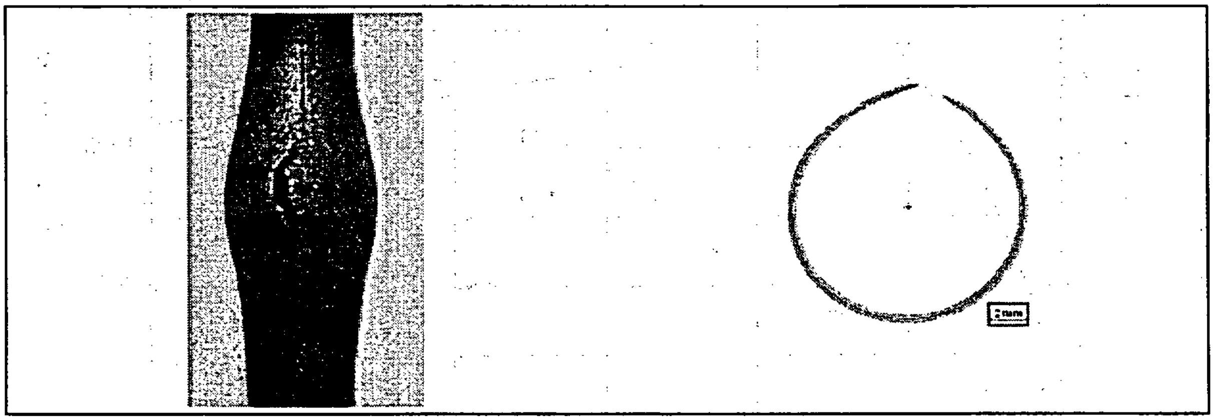

.Fig. 27. Cladding appearance and cross-section in burst area.

4.2.2. Calculation procedure and main results

FRAPTRAN calculations of these tests have been conducted with the purpose to verify the set of models, which describe ballooning and burst of Zr-1%Nb cladding. The calculations were conducted using boundary conditions of 1st type, i.e. using temperature versus time dependencies (as measured). Pressure drop at the cladding was assigned in the similar fashion (see Fig. 26). At that, in the last case linear extrapolation of the assigned pressure drop was conducted to the point of predicted burst of the cladding.

Main parameters of the simulators and initial data RIAR-LOCA2 test calculations are given in Table 18.

Table 18. Main parameters of simulator and initial data for LOCA calculations.

PARAMETER	UNITS	VALUE
Cladding	-	Zr-1%Nb
Fuel	-	Al_2O_3
Coolant	-	Argon
Cladding outside diameter	mm	9.1
Cladding inside diameter	mm	7.6
Cladding thickness	mm	0.7
Radial gap thickness	mm	0.03
Samples height	m	0.2

Results of cladding deformation and time to failure calculations are shown in Fig. 28, Fig. 29. Preliminary analysis of these results shows that predictions of cladding burst pressure – temperature and time to rupture were satisfactory. Calculated residual hoop strain of the cladding (43%) is also close to the experimental value (54%).

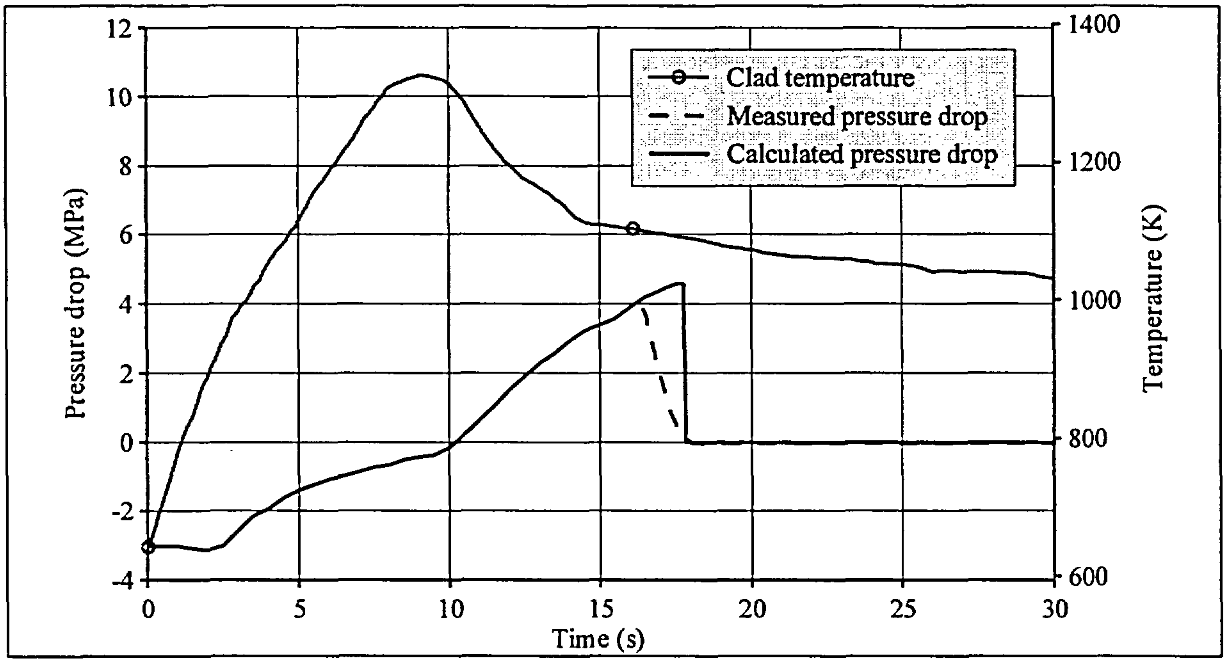

Fig. 28. Comparison of calculated and experimental values of failure pressure and temperature.

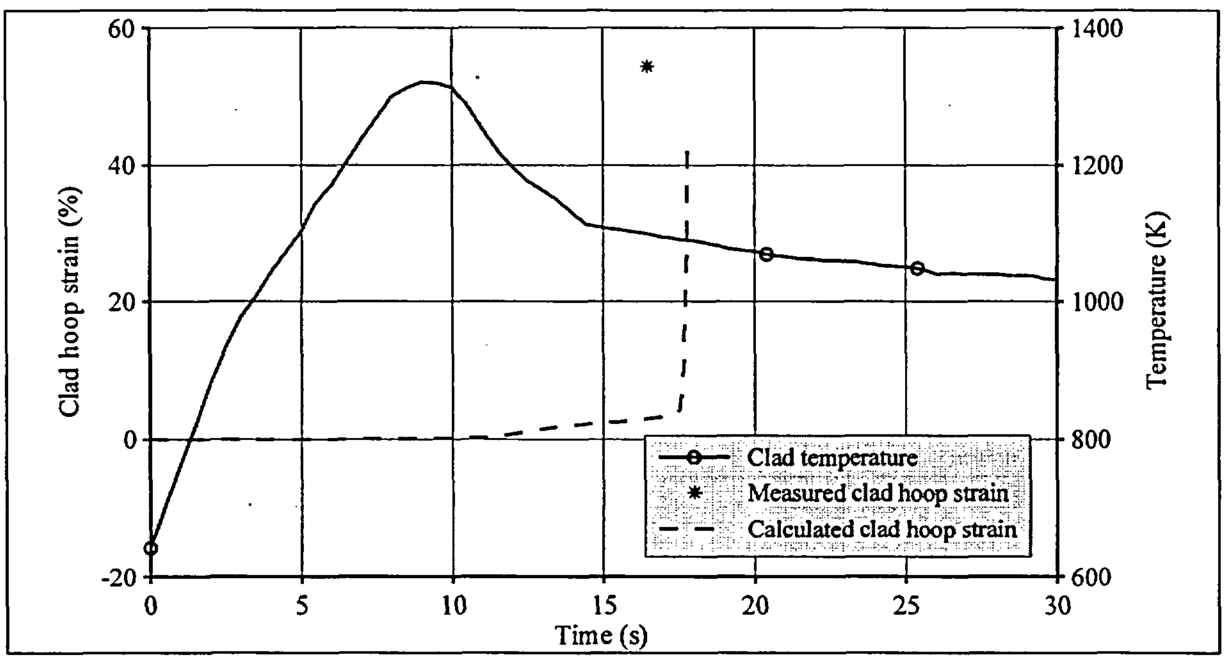

Fig. 29. Comparison of calculated and experimental values of cladding residual strain.

4.2.3. Summary of the assessment of the FRAPTRAN (modified) against LOCA-simulated test data

Comparison of experimental and calculated data in terms of parameters (pressure – temperature) of the fuel rod simulator failure is shown in Table 19.

Table 19. Comparison of experimental and calculated data on high-temperature cladding deformation under conditions modeling the first stage of LOCA.

Parameter	RIAR-LOCA2	
	experim.	calc.
Cladding rupture	Yes	Yes
Pressure drop during cladding failure (depressurization) (MPa)	3.88	4.57
Cladding temperature at the time of failure (depressurization) (K)	1099	1089
Time to failure (depressurization) (s) *	16.5	17.8
Maximum hoop strain (%)	54.4	42.9

As is seen from Table 19, these first calculations of behavior of the fuel rod simulator with unirradiated Zr-1%Nb cladding in the test, which imitates thermal and mechanical impact under LOCA conditions, revealed satisfactory match of calculated and experimental strength parameters of cladding rupture. Cladding failure criterion in the form of hoop stress at burst, which was implemented in MATPRO (see section 2.2), led to obtaining of reliable predictions of the cladding rupture time. At the same time, some underprediction of circumferencial strain at burst was obtained. Most likely, this is a reflection of a known problem of predicting maximum cladding deformation at burst. High sensitivity of this parameter to the loading conditions, which is revealed through wide dispersion of out-of-pile and in-pile test data, causes serious difficulties both in developing criterial correlations and in calculation modeling of cladding deformation process. Therefore, performance capabilities of the BALON2 subcode, which is used in FRAPTRAN for calculating local ballooning and rupture of the cladding, should be analyzed critically. Such analysis presents a separate task for the future and it should be accompanied by attempts to understand all accumulated test database on circumferencial elongation of cladding under LOCA conditions.

* Time calculated from the beginning of the test to the point of cladding failure (depressurization).

5. CONCLUSIONS

1. This study is a continuation of the series of works conducted at RRC KI in relation to adaptation of transient fuel rod behavior codes to analysis of behavior of fuel with Zr-Nb cladding. Due to its high operational performance, Zr-1%Nb (E110) cladding is considered as one of the most realistic candidates for high burnup fuel. Therefore, expansion of the area of application of these codes in the direction of safety analysis of fuel with alternative cladding (with respect to Zircaloy cladding) was the main objective of such activity. Accumulated earlier experience in modification and adaptation of NRC's FRAP-T6 and French IRSN's SCANAIR codes to behavioral analysis of fuel of Russian pressurized water reactor of VVER type under conditions of Reactivity Initiated Accident was the basis for conducting appropriate activities using new FRAPTRAN code developed by request of NRC.
2. As a result of intensive program on studying mechanical properties of unirradiated and highly irradiated Zr-1%Nb cladding initiated in 1996, expanded MATPRO package of material properties was developed for behavioral analysis of fuel with niobium cladding in joint use with thermal mechanical codes. Last updated version of the package presented in this report accumulated all testing and analytical results obtained to this date.
3. In addition to the development of expanded package of material properties, work on modification and adaptation of FRAPTRAN code was conducted in the scope necessary to perform calculations of selected RIA and LOCA assessment cases with fuel of VVER type. All models modified earlier for FRAP-T6 version designed for calculations of high burnup VVER fuel, have been transferred to FRAPTRAN. Significant scope of coding work due to introduction of new global and local variables as well as to correction of some inaccuracies and errors in the original code has been performed.
4. Three IGR power pulse tests with unirradiated rods (for which experimental records of cladding temperature and internal pressure are available) and three tests with high burnup commercial fuel have been modeled using modified FRAPTRAN code. Obtained results led to the following conclusions:

- Main thermal and mechanical parameters predicted by the code are in reasonable compliance with experimental data obtained with instrumented fresh fuel in wide range of peak enthalpy of the fuel and corresponding range of clad-to-coolant heat transfer modes.
- Main thermal and mechanical parameters of high burnup fuel rods H1T, H5T, H7T predicted by FRAPTRAN are also in satisfactory compliance with predictions of modified FRAP-T6 and SCANAIR codes obtained earlier and available post-test data.
- Certain systematic underestimation of peak enthalpy and overestimation of cladding temperature by the FRAPTRAN code has been observed as compared with previous data of modified FRAP-T6. Performed analysis revealed that these differences could be explained by different empirical coefficients in fuel-cladding gap thermal conductance models used in these codes.

5. Calculations of the selected LOCA assessment cases have been conducted using the modified FRAPTRAN code. Comprehensive out-of-pile test of the fuel rod simulator with unirradiated Zr-1%Nb cladding, during which thermal and mechanical cladding impacts simulated conditions of initial stage of LOCA, has been performed. Good agreement between calculated and experimental values was achieved for such parameters as pressure-temperature at burst, and time to failure. Satisfactory predictions of maximum hoop strain at burst (43% versus actual 55%) were obtained.
6. Very limited LOCA assessment does not allow for unambiguous conclusion about quality of prediction of maximum hoop strain at burst. However, taking into consideration known contradictions in the accumulated database on circumferential elongation of cladding under LOCA conditions and difficulties in modeling of ballooning, it should be mentioned that critical analysis of the entire existing test database needs to be performed and new approaches to prediction of maximum hoop strain need to be considered.

7. In general, based on experience with the above codes accumulated at RRC KI some general observations can be made in relation to the first version of FRAPTRAN, which was modified for high-burnup VVER fuel:

- the code is a new important step in development of the FRAP-T family codes. The issued first version of the FRAPTRAN code can serve as a basis for achieving up-to-date level of high-burnup fuel behavior modeling;
- from the user's standpoint, advantages of the new code include friendly service and convenient post-processing of the output data. Ease of using FORTRAN source and transparent procedure for preparation of initial data should also be noted;
- disadvantages of the analytical model include the requirement for the user to assign time step and unavailability of automatic selection of integration step in the process of calculation, which makes use of the code more difficult and time consuming;
- check of mechanical model of the code in analyzing behavior of the fuel with Zr-Nb cladding is of an interest for continuation of the code validation. For instance, results of the recent tests of VVER fuel (burnup 50–60 MWd/kg U) under conditions of narrow power pulses at BIGR reactor [1, 2] can be used for this purpose. Potential value of the results of IGR pulse tests with initial negative pressure drop on the cladding (16 MPa) should also be noted [2], since these initial conditions are more prototypical for full-scale reactor case.

8. From the standpoint of further enhancement of FRAPTRAN models of high-burnup fuel behavior, the following tasks are believed by the authors of the report to be a priority:

- re-assessment of boiling curve as applied to transient conditions of clad-to-coolant heat transfer typical for RIA;
- development of models of fission gas release, transient fuel swelling and formation of heterogeneous fuel structure (density, grain size) along the pellet radius;
- development of the model of mechanical interaction of fuel and cladding with consideration for irregularity of temperature fields and material properties.

9. The following priority tasks in development of models of Zr-1%Nb cladding material properties, implemented in MATPRO package should be considered:

- obtaining of continuous dependence of cladding mechanical properties vs. burnup;
- expansion of the range of studied burnup to 60 MWd/kg U and more;
- taking into account the effect of heating and cooling rates on phase transition temperatures and therefore on temperature dependencies of mechanical properties;
- adjustment of obtained correlations to account for annealing of radiation damages as a function of heating rate;
- development of approaches to possible extrapolation of obtained stress-strain data beyond the uniform elongation for adequate prediction of cladding deformation up to the failure.

References

[1] V.P.Smirnov, A.V.Smirnov, V.A.Tsykanov, Ye.G.Bek, A.K.Panioushkin, A.A. Enin, V.Rozhkov, "Characteristics of VVER fuel after operation at steady-state and transient conditions. Forecasting of ultra-high burnup". *Proceedings of Scientific&Technical Conference "Nuclear Power on the Threshold of XXI Century"*, 8-10 June 2000, Electrostal, Russia (rus).

[2] V.Asmolov, and L.Yegorova, "The Russian RIA Research Program: Motivation, Definition, Execution, and Results." Nuclear Safety, Vol.37, No 4, 1996.

[3] L.Yegorova, V.Asmolov, G.Abyshov, V.Malofeev, A.Avvakumov, E.Kaplar, K.Lioutov, A.Shestopalov, A.Bortash, L.Maiorov, K.Mikitiouk, V.Polvanov, V.Smirnov, A.Goryachev, V.Prokhorov, and A.Vurim, "Data Base on the Behaviour of High Burnup Fuel Rods with Zr-1%Nb Cladding and UO_2 Fuel (VVER Type) under Reactivity Initiated Accident Conditions", NUREG/IA-0156, (IPSN99/08-02, NSI/RRC KI 2179), Vol.1, 2, 3 1999.

[4] Yu.K.Bibilashvili, L.A.Yegorova, O.A.Nechaeva, I.G. Smirnov, V.P.Smirnov et.al., Experimental Study of VVER High Burnup Fuel Rods at the BIGR Reactor under Narrow Pulse Conditions. 2000 International Topical Meeting on Light Water Reactor Fuel Performance, Park City, Utah, April 10-13, 2000, pp.306-314.

[5] E.Kaplar, L.Yegorova, K.Lioutov, A.Konobeyev, N.Jouravkova, V.Smirnov, A.Goryachev, V.Prokhorov, O.Makarov, S.Yeremin, A.Svyatkin, "Mechanical properties of unirradiated and irradiated Zr-1%Nb cladding" NSI RRC 2241, NUREG/IA-0199, IPSN 01-16, April 2001.

[6] A.Shestopalov, K.Lioutov, L.Yegorova, G.Abyshov, K.Mikitiouk, "Modification of USNRC's FRAP-T6 Fuel Rod Transient Code for High Burnup VVER Fuel." NUREG/IA-0164, RRC KI 2180, IPSN 99/10 May 1999.

[7] K.Mikitiouk, A.Shestopalov, K.Lioutov, L.Yegorova, G.Abyshov, "Modification of IPSN's SCANAIR Fuel Rod Transient Code for High Burnup VVER Fuel." NUREG/IA-0165, RRC KI 2185, IPSN 99/09, May 1999.

[8] V.Asmolov, L.Yegorova, E.Kaplar, K.Lioutov, V.Smirnov, V.Prokhorov, and A.Goryachev, "Development of Data Base with Mechanical Properties of Un-and Preirradiated VVER cladding", *Proceedings of the 25th Water Reactor Safety Information Meeting*, Bethesda, Maryland, USA, NUREG/CP-0162, 1998.

[9] K. Lioutov, L. Yegorova, E. Kaplar, A. Konobeyev, V. Smirnov, A. Goryachev, V. Prokhorov, and S. Eremin, "Mechanical properties of unirradiated and irradiated Zr-1%Nb cladding under accident conditions", *Proceedings of the 27th Water Reactor Safety Information Meeting*, Bethesda, Maryland, USA, NUREG/CP-0169, 2000.

[10] L.Yegorova, K.Lioutov, E.Kaplar, "Overview of test results on mechanical properties of unirradiated and irradiated Zr-1%Nb (E-110 alloy) cladding" Proceedings of Nuclear Safety Research Conference Information Meeting, Washington, DC, October 22-24, 2001.

[11] M.E. Cunningham, C.E. Beyer, P.G. Medvedev, and G.A. Berna, "FRAPTRAN: A Computer Code for the Transient Analysis of Oxide Fuel Rods". NUREG/CR-6739 Vol.1 PNNL-13576, September 2001.

[12] D.D.Lanning, C.E.Beyer, C.L.Painter, "FRAPCON-3: Modifications to fuel rod material properties and performance models for high-burnup application". NUREG/CR-6534 Vol.1 PNNL-11513, December 1997.

[13] B.Yu.Volkov et al., Material property library for H-1 alloy cladding, Report IAE-4941/11, 1989.

[14] Ljusternik V.E., Peletski V.E., Petrova I.I. "Experimental research of zirconium reactor materials thermal properties. Zr+1%Nb alloy." M., J. High Temperature Thermal Physics. v. 31, N4, 1993. (rus).

[15] V.S. Chirkin, "Thermal-physical properties of nuclear materials", Atomizdat, Moscow, 1968. (rus).

[16] A.S.Zaimovskyi, A.V.Nikulina, N.G.Reshetnikov, "Zirconium Alloys in the Nuclear Industry". Moscow, Energoizdat, 1981 (rus).

[17] D.L.Hagrman, G.A.Reymann, R.E.Mason "MATPRO-Version 11 (revision 1): A Handbook of Material Properties for Use in the Analysis of Light Water Reactor Fuel Rod Behavior", NUREG/CR-0497, Rev 1, February 1980.

[18] Pirogov Ye.N., Alimov M.I., Artiuchina L.L., "Creep of H-1 alloy in the range of phase transition", Journal of Atomnaya energiya, v.65 (3), p. 293, 1988. (rus).

[19] G.P.Kobyliansky, A.Ye.Novoselov, "Radiation Tolerance of Zirconium and Zirconium-Based Alloys", Edited by V.A.Tsycanov. Dimitrovgrad: State Research Centre of Russian Federation NIIAR, 1996 (rus)

[20] L. Baker and L.C. Just, Studies of metal-water reactions at high temperatures, ANL-6548 (1962).

[21] J.V. Cathcart, et al., Zirconium Metal-Water Oxidation Kinetics IV. Reaction Rate Studies, *ORNL/NUREG-17, 1977.*

[22] Yu.K. Bibilashvili, N.B. Sokolov, L.N. Andreyeva-Andrievskaya, A.V. Salatov , A.M. Morozov, High-temperature Interaction of Fuel Rod Cladding Material (Zr-1%Nb alloy) with Oxygen-containing Mediums. *Proceedings of IAEA Technical Committee on Behaviour of LWR Core Materials under Accident Conditions,* Dimitrovgrad, Russia, on 9-13 October 1995, IAEA-TEC-DOC-921, Vienna, 1996, pp. 117-128.

[23] M. L. Pomeranz, "Film Boiling on a Horizontal Tube in Increased Gravity Fields," *Journal of Heat Transfer, 86,* (1974) pp. 213-219.

[24] A.Labuntzov, Teploenergetika. 12 (1959), Russia (rus), pp. 19-26.

[25] S.S.Kutateladze, Fundamentals of Heat Transfer Theory, M., Atomizdat, 1979.

[26] G.N. Poletaev, "Analytical equations for approximate analysis of fuel rod rewetting in reactivity initiated accidents", Report IAE-6090/5, 1998.

[27] «RELAP5/MOD3: Code Manual. Volume IV: Models and Correlations», NUREG/CR-5535, INEL-95/0174.

[28] D.D.Lanning, C.E.Beyer, C.L.Painter, "FRAPCON-3: Modifications to fuel rod material properties and performance models for high-burnup application". NUREG/CR-6534 Vol.1 Pnnl-11513, December 1997.

[29] V.Smirnov, A.Smirnov, V. Tsycanov, V. Asmolov, L. Yegorova, L. Andreeva-Andrievskaya, Yu. Bibilashvili, B. Sokolov, Eu. Bek, A. Panjushkin, and V. Ryabov, "The Results of Experimental Studies on the Behavior of High Burnup Fuel of Pressurized Water Reactors in Loss-of-Coolant Accidents", *Proceedigns of Scientific&Technical Conference "Nuclear Power on the Threshold of XXI Century"*, 8-10 June 2000, Electrostal, Russia (rus).

[30] M.E.Cunningham, C.E.Beyer, F.E.Panisko, P.G.Medvedev, G.A.Berna, H.H.Scott, "FRAPTRAN: Integral assessement". NUREG/CR-6739 Vol.2 PNNL-13576, September 2001.

[31] M.Vostrikov, B.Kochurov, "TRIFOB - the Code for Calculation of Isotopic Composition in a Cylindrical Reactor Cell Taking into Account Neutron Spatial-Energy Distribution", Rus., Report ITEP-106, Moscow, 1981.

[32] F. Lamare, J.C. Latche, "SCANAIR. A Computer Code for Reactivity Initiated Accidents in LWRs", Rapport Technique SEMAR 95/01.

[33] Yu.K.Bibilashvili, L.A.Yegorova, O.A.Nechaeva, I.G. Smirnov, V.P.Smirnov et.al., "Experimental Study of VVER High Burnup Fuel Rods at the BIGR Reactor under Narrow Pulse Conditions." *International Topical Meeting on Light Water Reactor Fuel Performance,* Park City, Utah, April 10-13, 2000, pp.306-314.

[34] Yu.Bibilashvili, A.Goryachev, O.Nechaeva, A.Salatov, V.Sazhnov, I.Smirnov, N.Sokolov, Yu.Trutnev, V.Ustinenko, L.Yegorova, "Study of High Burnup VVER Fuel Rods Behavior at the BIGR Reactor under RIA Conditions: Experimental Results". *OECD RIA Topical Meeting, CABRI Seminar (opened part),* Aix-en-Provance, France, May 13, 2002.

NRC FORM 335
(2-89)
NRCM 1102,
3201, 3202

U.S. NUCLEAR REGULATORY COMMISSION

BIBLIOGRAPHIC DATA SHEET

(See instructions on the reverse)

1. REPORT NUMBER
(Assigned by NRC, Add Vol., Supp., Rev., and Addendum Numbers, if any.)

NUREG/IA-0209
NSI RRC KI 3067
IRSN-2002/33

2. TITLE AND SUBTITLE

Adaptation of USNRC's FRAPTRAN and IRSN's SCANAIR Transient Codes and Updating of MATPRO Package for Modeling of LOCA and RIA Validation Cases with Zr-1% Nb (VVER type) Cladding

3. DATE REPORT PUBLISHED

MONTH	YEAR
April	2003

4. FIN OR GRANT NUMBER

Y6723

5. AUTHOR(S)

A. Shestopalov, K. Lioutov, L. Yegorova

6. TYPE OF REPORT

7. PERIOD COVERED *(Inclusive Dates)*

2001-2002

8. PERFORMING ORGANIZATION - NAME AND ADDRESS *(If NRC, provide Division, Office or Region, U.S. Nuclear Regulatory Commission, and mailing address; if contractor, provide name and mailing address.)*

Russian Research Center - Kurchatov Institute
Moscow 123182
Russia

9. SPONSORING ORGANIZATION - NAME AND ADDRESS *(If NRC, type "Same as above"; if contractor, provide NRC Division, Office or Region, U.S. Nuclear Regulatory Commission, and mailing address.)*

Division of Systems Analysis and Regulatory Effectiveness
Office of Nuclear Regulatory Research
U.S. Nuclear Regulatory Commission
Washington, DC 20555-001

10. SUPPLEMENTARY NOTES

11. ABSTRACT *(200 words or less)*

The report presents the results of analytical work on updating and supplementing Zr-1%Nb (E110) cladding material property models as part of MATPRO package intended for joint use with thermal mechanical codes analyzing high burnup fuel transient behavior. The scope of work also included adapting U.S.NRC's FRAPTRAN code to the behavior analysis of fuel with E110 cladding (VVER type) and carrying out of the code assessment using selected experimental data. Satisfactory compliance of the results calculated by modified FRAPTRAN version with in-pile RIA and out-of-pile LOCA simulated test results is obtained. The obtained calculation data have been also compared with the predictions of the FRAP-T6 (U.S.NRC) and SCANAIR (IRSN, France) codes modified earlier.

12. KEY WORDS/DESCRIPTORS *(List words or phrases that will assist researchers in locating the report.)*

reactivity initiated accident
cladding-to-coolant heat transfer model
SCANAIR computer code
material properties
cladding strain and ballooning
code assessment

13. AVAILABILITY STATEMENT

unlimited

14. SECURITY CLASSIFICATION

(This Page)
unclassified

(This Report)
unclassified

15. NUMBER OF PAGES

16. PRICE

UNITED STATES
NUCLEAR REGULATORY COMMISSION
WASHINGTON, DC 20555-0001

OFFICIAL BUSINESS